

SUPPLEMENTARY INFORMATION

Opposing Roles of Hepatic Stellate Cell Subpopulations in Hepatocarcinogenesis

Aveline Filliol¹, Yoshinobu Saito^{1†}, Ajay Nair^{1,2†}, Dianne Dapito^{1†}, Le-Xing Yu^{1†}, Aashreya Ravichandra¹, Sonakshi Bhattacharjee¹, Silvia Affo¹, Naoto Fujiwara⁶, Hua Su⁷, Qiuyan Sun¹, Thomas M Savage⁸, John R Wilson-Kanamori³, Jorge M Caviglia¹, LiKang Chin⁴, Dongning Chen⁴, Xiaobo Wang¹, Stefano Caruso⁵, Jin Ku Kang^{1,9}, Amit Dipak Amin¹, Sebastian Wallace³, Ross Dobie³, Deqi Yin¹, Oscar M Rodriguez-Fiallos¹, Chuan Yin¹, Adam Mehal¹, Benjamin Izar¹, Richard A. Friedman¹⁰, Rebecca G. Wells⁴, Utpal B. Pajvani^{1,9}, Yujin Hoshida⁶, Helen Remotti¹¹, Nicholas Arpaia⁸, Jessica Zucman-Rossi⁵, Michael Karin⁷, Neil C Henderson^{3,13}, Ira Tabas^{1,9,11,12}, Robert F. Schwabe^{1,9*}

Affiliations:

¹ Department of Medicine, Columbia University, New York, NY 10032, USA.

² Department of Systems Biology, Columbia University Irving Medical Center, New York, NY 10032, USA.

³ Centre for Inflammation Research, The Queen's Medical Research Institute, Edinburgh BioQuarter, University of Edinburgh, Edinburgh EH16 4TJ, UK.

⁴ Perelman School of Medicine, University of Pennsylvania, Philadelphia, PA 19104, USA

⁵ Centre de Recherche des Cordeliers, INSERM, Sorbonne Université, Université de Paris, Functional Genomics of Solid Tumors Laboratory, Paris, France.

⁶ Liver Tumor Translational Research Program, Harold C. Simmons Comprehensive Cancer Center, Division of Digestive and Liver Diseases, University of Texas Southwestern Medical Center, Dallas, TX 75390, USA.

⁷ Department of Pharmacology, School of Medicine, University of California, San Diego, San Diego, CA, USA

⁸ Department of Microbiology & Immunology, Columbia University Irving Medical Center, New York, NY USA

⁹ Institute of Human Nutrition, New York, NY 10032, USA.

¹⁰ Biomedical Informatics Shared Resource, Herbert Irving Comprehensive Cancer Center, and Department of Biomedical Informatics, Columbia University Irving Medical Center, New York, NY 10032, USA.

¹¹ Department of Pathology, Columbia University Irving Medical Center, New York, NY 10032, USA.

¹² Department of Physiology, Columbia University, New York, NY 10032, USA.

¹³ MRC Human Genetics Unit, Institute of Genetics and Cancer, University of Edinburgh, Edinburgh, UK.

* Correspondence to: Robert F. Schwabe, 1130 St.Nicholas Ave, ICRC, Room 926, New York, NY 10032; phone: 212-851-5462; rfs2102@cumc.columbia.edu

TABLE OF CONTENTS

SUPPLEMENTARY TABLES

Supplementary Table 1| GO biological process enrichment pathway analysis of hepatocyte subclusters C10 (a) and C13 (b). Table related to Extended Data Figure 4f. Adj_p.value: adjusted p.value.

Supplementary Table 2| Full Mouse myHSC gene signature. myHSC signature genes, sorted by average log-fold change (Avg_logFC) between highly and less activated HSC clusters from which the signature were derived, with positive values indicate that the genes are more highly expressed in the activated HSC. Genes encoding for a secreted protein were determined using Uniprot and Protein Atlas databases. p_val_adj: Adjusted p-value.

Supplementary Table 3| Full Mouse cyHSC gene signature. cyHSC signature genes, sorted by average log-fold change (Avg_logFC) between highly and less activated HSC clusters from which the signature were derived, higher negative values mark the genes that more highly expressed in the less activated HSC. Genes encoding for a secreted protein were determined using Uniprot and Protein Atlas databases. p_val_adj: Adjusted p-value.

Supplementary Table 4| GO biological process enrichment pathway analysis showing the top biological processes for mouse myHSC (a) and cyHSC (b) signatures. adj_p.value: adjusted p.value.

Supplementary Table 5| Top 25 genes encoding secreted proteins in myHSC (a) and cyHSC (b) subpopulations, determined by the signatures generated in Supplementary Information 3. avg_log2FC: average log2 fold change; adj_p.value: adjusted p.value.

Supplementary Table 6| cyHSC (a) and myHSC (b) genes used to determine cyHSC-myHSC balance in patient cohorts. The Avg_logFC: log fold-change of the average expression between highly and less activated HSC. Positive values indicate that the genes are more highly expressed in the highly activated HSC, negative values indicate that the genes are highly expressed in the less activated HSC. p_val_adj : adjusted p- value.

Supplementary Table 7| Summarize of all mouse HCC models used in this study. ND: not determined.

Supplementary Table 8| Summarize of proliferation and cell death analysis performed in this study.

SUPPLEMENTARY DATA

Supplementary Information 1| Single nucleus RNA-sequencing analysis of human normal, fibrotic and HCC liver tissues.

Supplementary Information 2 | Immune cell analysis by flow cytometry in the fibrotic liver or HCC from mice with genetic HSC depletion or inhibition.

Supplementary Information 3 | Strategy to generate a single cell RNA-sequencing signature for weakly and strongly activated HSC subpopulations.

Supplementary Information 4| Immune cell analysis by flow cytometry in the fibrotic liver or HCC from mice with genetic deletion of *Collal* in HSC

Supplementary Information 5| Immune cell analysis by flow cytometry in CCl₄-induced liver injury in the fibrotic liver from mice with deletion of *Hgf* in HSC.

Supplementary Information 6| Uncropped immunoblots from Main Figures 4f (a) and Mine Figure 5a (b).

Supplementary Information 7| Uncropped immunoblots from Main Figure 5e (a), Main Figure 5f (b) and Extended Data Figure 2g (c).

Supplementary Information 8| Uncropped immunoblots from Extended Data Figure 10b (a) and Extended Data Figure 10e (b).

Supplementary Information 9| Uncropped immunoblots from Extended Data Figure 10f (a) and Extended Data Figure 10g (b).

Supplementary Information 10| Uncropped immunoblots from Extended Data Figure 10j.

Supplementary Table 1. GO biological process enrichment pathway analysis of hepatocyte subclusters C10 (a) and C13 (b). Table related to Extended Data Figure 4f. Adj_p.value: adjusted p.value.

a. Hepatocyte subcluster C10

| Pathways | Genes (n)/ all genes (n) | p.value | Adj_p.value |
|--|--------------------------|-------------|-------------|
| mitotic cell cycle (GO:0000278) | 14/404 | 4.8E-14 | 3.1E-11 |
| cytokinesis (GO:0000910) | 7/79 | 2.8E-10 | 0.000000045 |
| regulation of cell cycle process (GO:0010564) | 11/481 | 0.000000003 | 0.00000028 |
| cell cycle checkpoint (GO:0000075) | 7/156 | 0.000000033 | 0.0000016 |
| positive regulation of ubiquitin-protein transferase activity (GO:0051443) | 5/87 | 0.000001 | 0.000026 |
| positive regulation of ligase activity (GO:0051351) | 5/92 | 0.0000014 | 0.000032 |
| positive regulation of cell cycle process (GO:0090068) | 5/220 | 0.000094 | 0.00078 |
| protein folding (GO:0008457) | 5/221 | 0.000096 | 0.00079 |
| modification-dependent macromolecule catabolic process (GO:0043632) | 5/368 | 0.001 | 0.0057 |
| negative regulation of protein catabolic process (GO:0042177) | 3/97 | 0.0011 | 0.0061 |
| negative regulation of cytoskeleton organization (GO:0051494) | 3/101 | 0.0012 | 0.0068 |
| regulation of muscle tissue development (GO:1901861) | 3/113 | 0.0017 | 0.0087 |
| guanosine-containing compound catabolic process (GO:1901069) | 4/246 | 0.0017 | 0.0087 |
| hyaluronan metabolic process (GO:0030212) | 2/31 | 0.0019 | 0.0092 |

b. Hepatocyte subcluster C13

| Pathways | Genes (n)/ all genes (n) | p.value | Adj_p.value |
|--|--------------------------|----------|-------------|
| response to progesterone (GO:0032570) | 4/33 | 0.000022 | 0.011 |
| cellular response to calcium ion (GO:0071277) | 4/38 | 0.000038 | 0.011 |
| phosphatidylethanolamine biosynthetic process (GO:0006646) | 3/14 | 0.000042 | 0.011 |
| transforming growth factor beta receptor signaling pathway (GO:0007179) | 6/134 | 0.000058 | 0.011 |
| cellular response to transforming growth factor beta stimulus (GO:0071560) | 6/166 | 0.00019 | 0.018 |
| response to starvation (GO:0042594) | 5/106 | 0.00019 | 0.018 |
| response to nutrient levels (GO:0031667) | 7/291 | 0.00065 | 0.042 |
| carbohydrate homeostasis (GO:0033500) | 5/143 | 0.00076 | 0.042 |
| glucose homeostasis (GO:0042593) | 5/143 | 0.00076 | 0.042 |
| glucose metabolic process (GO:0006006) | 5/149 | 0.00092 | 0.043 |

Supplementary Table 2. Full Mouse myHSC gene signature. myHSC signature genes, sorted by average log-fold change (Avg_logFC) between highly and less activated HSC clusters from which the signature were derived, with positive values indicate that the genes are more highly expressed in the activated HSC. Genes encoding for a secreted protein were determined using Uniprot and Protein Atlas databases. p_val_adj: Adjusted p-value.

| Rank | Gene name | Gene ID | Description | avg_logFC | p_val_adj | Secreted (UniProt) |
|------|-----------|-----------|--|-------------|-----------|--------------------|
| 1 | Spp1 | 20750 | secreted phosphoprotein 1 | 4.114145131 | 0 | yes |
| 2 | Mgp | 17313 | matrix Gla protein | 3.628214502 | 0 | yes |
| 3 | S100a6 | 20200 | S100 calcium binding protein A6 | 3.090263886 | 0 | |
| 4 | Timp1 | 21857 | TIMP metallopeptidase inhibitor 1 | 3.02414586 | 0 | yes |
| 5 | Serpine2 | 20720 | serpin family E member 2 | 3.010402684 | 0 | yes |
| 6 | Ptn | 19242 | pleiotrophin | 2.484395056 | 0 | yes |
| 7 | Col15a1 | 12819 | collagen type XV alpha 1 chain | 2.449939885 | 0 | yes |
| 8 | Col1a1 | 12842 | collagen type I alpha 1 chain | 2.447026237 | 0 | yes |
| 9 | Eln | 13717 | elastin | 2.426745974 | 0 | yes |
| 10 | Lpl | 16956 | lipoprotein lipase | 2.380721258 | 0 | yes |
| 11 | Fxyd6 | 59095 | FXYD domain containing ion transport regulator 6 | 2.215368349 | 0 | |
| 12 | Ltbp2 | 16997 | latent transforming growth factor beta binding protein 2 | 2.103696756 | 0 | yes |
| 13 | Dpt | 56429 | dermatopontin | 1.95931803 | 0 | yes |
| 14 | Col1a2 | 12843 | collagen type I alpha 2 chain | 1.894798899 | 0 | yes |
| 15 | Lgals1 | 16852 | galectin 1 | 1.831543817 | 0 | yes |
| 16 | Serpina3n | 20716 | serpin family A member 3 | 1.819088561 | 0 | yes |
| 17 | Mfap4 | 76293 | microfibril associated protein 4 | 1.787033453 | 0 | yes |
| 18 | Emp1 | 13730 | epithelial membrane protein 1 | 1.767814006 | 0 | |
| 19 | Sparc1 | 13602 | SPARC like 1 | 1.731738413 | 0 | yes |
| 20 | Htra1 | 56213 | HtrA serine peptidase 1 | 1.685952809 | 0 | yes |
| 21 | Fbn2 | 14119 | fibrillin 2 | 1.673157506 | 0 | yes |
| 22 | Cd34 | 12490 | CD34 molecule | 1.659823447 | 0 | |
| 23 | Tnc | 21923 | tenascin C | 1.59174016 | 0 | yes |
| 24 | Timp3 | 21859 | TIMP metallopeptidase inhibitor 3 | 1.575243024 | 0 | yes |
| 25 | Plat | 18791 | plasminogen activator, tissue type | 1.572147289 | 0 | yes |
| 26 | Fzd1 | 14362 | frizzled class receptor 1 | 1.531259919 | 0 | |
| 27 | Col6a3 | 12835 | collagen type VI alpha 3 chain | 1.528521617 | 0 | yes |
| 28 | Igf1 | 16000 | insulin like growth factor 1 | 1.494235809 | 0 | yes |
| 29 | Lox11 | 16949 | lysyl oxidase like 1 | 1.458796533 | 0 | yes |
| 30 | Ncam1 | 17967 | neural cell adhesion molecule 1 | 1.439169518 | 0 | yes |
| 31 | Crip1 | 12925 | cysteine rich protein 1 | 1.39097808 | 0 | |
| 32 | Acta2 | 11475 | actin alpha 2, smooth muscle | 1.374724426 | 5.46E-250 | |
| 33 | Gas6 | 14456 | growth arrest specific 6 | 1.365753972 | 0 | yes |
| 34 | Col8a1 | 12837 | collagen type VIII alpha 1 chain | 1.318805635 | 5.73E-287 | yes |
| 35 | Col5a2 | 12832 | collagen type V alpha 2 chain | 1.294930587 | 0 | yes |
| 36 | Itgb5 | 16419 | integrin subunit beta 5 | 1.293146157 | 0 | |
| 37 | Ptgis | 19223 | prostaglandin I2 synthase | 1.28151658 | 0 | |
| 38 | Idr2 | 100039795 | immunoglobulin like domain containing receptor 2 | 1.270978435 | 0 | |
| 39 | S100a16 | 67860 | S100 calcium binding protein A16 | 1.270768034 | 0 | |
| 40 | Lox | 16948 | lysyl oxidase | 1.265524707 | 0 | yes |
| 41 | Slc7a2 | 11988 | solute carrier family 7 member 2 | 1.239746621 | 0 | |
| 42 | Col4a5 | 12830 | collagen type IV alpha 5 chain | 1.202458835 | 0 | yes |
| 43 | Cxcl14 | 57266 | C-X-C motif chemokine ligand 14 | 1.189068683 | 4.61E-112 | yes |
| 44 | Mfap2 | 17150 | microfibril associated protein 2 | 1.177496807 | 0 | yes |
| 45 | Col3a1 | 12825 | collagen type III alpha 1 chain | 1.176094148 | 0 | yes |
| 46 | Colec12 | 140792 | collectin subfamily member 12 | 1.175105909 | 0 | |
| 47 | Fstl1 | 14314 | follistatin like 1 | 1.157727505 | 0 | yes |
| 48 | Adcy7 | 11513 | adenylyl cyclase 7 | 1.115955055 | 0 | |
| 49 | Mdk | 17242 | midkine | 1.092427577 | 2.47E-260 | yes |
| 50 | Fam180a | 208164 | family with sequence similarity 180 member A | 1.088779238 | 0 | yes |
| 51 | Runx1 | 12394 | RUNX family transcription factor 1 | 1.076976179 | 0 | |
| 52 | Ppi | 19038 | peptidylprolyl isomerase C | 1.072636963 | 0 | |
| 53 | Mtch1 | 56462 | mitochondrial carrier 1 | 1.07225673 | 0 | |
| 54 | Pdgfrl | 68797 | platelet derived growth factor receptor like | 1.071376115 | 0 | yes |
| 55 | Aebp1 | 11568 | AE binding protein 1 | 1.058994876 | 0 | yes |
| 56 | Col5a2 | 12834 | collagen type VI alpha 2 chain | 1.049962532 | 0 | yes |
| 57 | Pla1a | 85031 | phospholipase A1 member A | 1.0457689 | 0 | yes |
| 58 | Crispld2 | 78892 | cysteine rich secretory protein LCCL domain containing 2 | 1.04445127 | 1.01E-261 | yes |
| 59 | Igfbp4 | 16010 | insulin like growth factor binding protein 4 | 1.035744403 | 5.66E-144 | yes |
| 60 | Mmp2 | 17390 | matrix metallopeptidase 2 | 1.007010061 | 6.98E-212 | yes |
| 61 | Tgfr2 | 21813 | transforming growth factor beta receptor 2 | 1.005549193 | 5.00E-283 | |
| 62 | F2r | 14062 | coagulation factor II thrombin receptor | 0.99450768 | 2.28E-285 | |
| 63 | Aldh1a2 | 19378 | aldehyde dehydrogenase 1 family member A2 | 0.983828359 | 2.32E-307 | |
| 64 | Ak1 | 11636 | adenylyl kinase 1 | 0.974637329 | 0 | |
| 65 | Fhl2 | 14200 | four and a half LIM domains 2 | 0.940427423 | 1.20E-176 | |
| 66 | Nrep | 27528 | neuronal regeneration related protein | 0.93669654 | 0 | |
| 67 | Gsn | 227753 | gelsolin | 0.923846163 | 2.53E-195 | yes |
| 68 | Lrrna | 16905 | lamin A/C | 0.91507187 | 2.41E-278 | |
| 69 | Dpysl3 | 22240 | dihydropyrimidinase like 3 | 0.898209662 | 4.10E-288 | |
| 70 | Tbbs1 | 21825 | thrombospondin 1 | 0.885653089 | 1.07E-116 | yes |
| 71 | Sec61b | 66212 | SEC61 translocon subunit beta | 0.880221882 | 0 | |
| 72 | Tgfb3 | 21809 | transforming growth factor beta 3 | 0.864277977 | 9.04E-281 | yes |
| 73 | Col8a1 | 12833 | collagen type VIII alpha 1 chain | 0.86257709 | 2.13E-255 | yes |
| 74 | Mmp14 | 17387 | matrix metallopeptidase 14 | 0.858424048 | 2.27E-243 | |
| 75 | Serph1n | 12406 | serpin family H member 1 | 0.847637822 | 0 | |
| 76 | Phldb2 | 208177 | pleckstrin homology like domain family B member 2 | 0.840190124 | 2.99E-255 | |
| 77 | S100a4 | 20198 | S100 calcium binding protein A4 | 0.82356282 | 2.78E-238 | yes |
| 78 | Fkbp11 | 66120 | FKBP prolyl isomerase 11 | 0.818051228 | 8.94E-285 | |
| 79 | Ctsk | 13038 | cathepsin K | 0.808683453 | 8.27E-193 | |
| 80 | Nme2 | 18103 | NME/NM23 nucleoside diphosphate kinase 2 | 0.806714078 | 0 | |
| 81 | Tubb2a | 22151 | tubulin beta 2A class IIa | 0.784951632 | 6.64E-176 | |
| 82 | Sec61g | 20335 | SEC61 translocon subunit gamma | 0.767542823 | 0 | |
| 83 | Kdelr3 | 105785 | KDEL endoplasmic reticulum protein retention receptor 3 | 0.766818808 | 1.13E-234 | |
| 84 | Prepaa1 | 66112 | prostate transmembrane protein, androgen induced 1 | 0.733425609 | 8.73E-161 | |
| 85 | Cimp | 71566 | CXADR like membrane protein | 0.730978746 | 6.57E-225 | |
| 86 | Vamp5 | 53620 | vesicle associated membrane protein 5 | 0.721172763 | 9.70E-179 | |
| 87 | Hivep3 | 16656 | HIVEP zinc finger 3 | 0.714786039 | 9.83E-214 | |
| 88 | Abrac1 | 73112 | ABRA C-terminal like | 0.682481265 | 2.34E-169 | |
| 89 | Vim | 22352 | vimentin | 0.671159676 | 8.94E-273 | |
| 90 | S100a13 | 20196 | S100 calcium binding protein A13 | 0.653698021 | 4.94E-156 | yes |

Supplementary Table 3. Full Mouse cyHSC gene signature. cyHSC signature genes, sorted by average log-fold change (Avg_logFC) between highly and less activated HSC clusters from which the signature were derived, higher negative values mark the genes that more highly expressed in the less activated HSC. Genes encoding for a secreted protein were determined using Uniprot and Protein Atlas databases. p_val_adj: Adjusted p-value.

| Rank | Gene name | Gene ID | Description | avg_logFC | p_val_adj | Secreted (UniProt) |
|------|-----------|-----------|---|------------|---------------|--------------------|
| 1 | Rgs5 | 19737 | regulator of G-protein signaling 5 | 3.86379034 | 0 | |
| 2 | Colec11 | 71693 | collectin sub-family member 11 | 3.48463255 | 0 yes | |
| 3 | Angptl6 | 70726 | angiopoietin-like 6 | 3.18906662 | 0 yes | |
| 4 | Tmem56 | 99887 | TLC domain containing 4 | 2.98012069 | 0 | |
| 5 | Ecm1 | 13601 | extracellular matrix protein 1 | 2.87976026 | 0 yes | |
| 6 | Ifitm1 | 68713 | interferon induced transmembrane protein 1 | 2.73895669 | 0 | |
| 7 | Fcna | 14133 | fcnol A | 2.58345153 | 0 yes | |
| 8 | Lrat | 79235 | lecithin-retinol acyltransferase (phosphatidylcholine-retinol-O-acyltransferase) | 2.57189395 | 0 | |
| 9 | Colec10 | 239447 | collectin sub-family member 10 | 2.50084448 | 0 yes | |
| 10 | Refnl | 19699 | reelin | 2.49582687 | 0 yes | |
| 11 | Abcc9 | 20928 | ATP-binding cassette, sub-family C (CFTR/MRP), member 9 | 2.29933836 | 0 | |
| 12 | Masp1 | 17174 | mannan-binding lectin serine peptidase 1 | 2.2795445 | 0 yes | |
| 13 | Cxcl12 | 20315 | chemokine (C-X-C motif) ligand 12 | 2.2460276 | 0 yes | |
| 14 | Steap4 | 117167 | STEAP family member 4 | 2.23221491 | 0 | |
| 15 | Sod3 | 20657 | superoxide dismutase 3, extracellular | 2.21699214 | 0 yes | |
| 16 | Vipr1 | 22354 | vasoactive intestinal peptide receptor 1 | 2.19197056 | 0 | |
| 17 | Plvap | 84094 | plasma/lemma vesicle associated protein | 2.19036245 | 0 | |
| 18 | Col14a1 | 12818 | collagen, type XIV, alpha 1 | 2.18832234 | 0 yes | |
| 19 | Gdf2 | 12165 | growth differentiation factor 2 | 2.15696441 | 0 yes | |
| 20 | Dcn | 13179 | decorin | 2.13271758 | 0 yes | |
| 21 | Igfbp3 | 16009 | insulin-like growth factor binding protein 3 | 2.01729631 | 0 yes | |
| 22 | Ehd3 | 57440 | EH-domain containing 3 | 2.00394816 | 0 | |
| 23 | Wfdc1 | 67866 | WAP four-disulfide core domain 1 | 1.9894788 | 0 yes | |
| 24 | Tgfb1 | 21810 | transforming growth factor, beta induced | 1.97830906 | 0 yes | |
| 25 | Mustn1 | 66175 | musculoskeletal, embryonic nuclear protein 1 | 1.9743773 | 0 | |
| 26 | Nrxn1 | 18189 | neurexin I | 1.91565487 | 0 | |
| 27 | Rspo3 | 72780 | R-spondin 3 | 1.88929255 | 0 yes | |
| 28 | Ramp1 | 51801 | receptor (calcitonin) activity modifying protein 1 | 1.88782189 | 0 | |
| 29 | Pth1r | 19228 | parathyroid hormone 1 receptor | 1.80852442 | 0 | |
| 30 | Agr1r1a | 11607 | angiotensin II receptor, type 1a | 1.73882408 | 0 | |
| 31 | Rasgrp2 | 19396 | RAS, guanyl releasing protein 2 | 1.68942325 | 0 | |
| 32 | Cc2 | 20296 | chemokine (C-C motif) ligand 2 | 1.68778743 | 6.88E-162 yes | |
| 33 | Gos2 | 14373 | GU/G1 switch gene 2 | 1.67361138 | 0 | |
| 34 | H2-D1 | 14964 | histocompatibility 2, D region locus 1 | 1.66476896 | 0 | |
| 35 | Hs3t3b1 | 54710 | heparan sulfate (glucosamine)-3-O-sulfotransferase 3B1 | 1.66074412 | 0 | |
| 36 | Cica3a1 | 12722 | chloride channel accessory 3A1 | 1.66027626 | 0 | |
| 37 | Hgf | 15234 | hepatocyte growth factor | 1.64050577 | 0 yes | |
| 38 | Prepl | 116847 | proline arginine-rich end leucine-rich repeat | 1.63022931 | 0 yes | |
| 39 | Ednrb | 13618 | endothelin receptor type B | 1.62466016 | 0 | |
| 40 | Zfp36 | 22695 | zinc finger protein 36 | 1.60501943 | 0 | |
| 41 | Ppp1r14a | 68458 | protein phosphatase 1, regulatory inhibitor subunit 14A | 1.58754779 | 0 | |
| 42 | Hsd11b1 | 15483 | hydroxysteroid 11-beta dehydrogenase 1 | 1.58033222 | 0 | |
| 43 | Kcnj8 | 16523 | potassium inwardly-rectifying channel, subfamily J, member 8 | 1.55212043 | 0 | |
| 44 | SEPT4 | 18952 | septin 4 | 1.49037601 | 0 | |
| 45 | Aard | 239435 | alanine and arginine rich domain containing protein | 1.44812764 | 0 | |
| 46 | Arvcf | 11877 | armadillo repeat gene deleted in velocardiofacial syndrome | 1.40735682 | 0 | |
| 47 | Ferm2 | 218952 | fermitin family member 2 | 1.3967847 | 0 | |
| 48 | Bmp5 | 12160 | bone morphogenetic protein 5 | 1.39414604 | 0 yes | |
| 49 | Tnfrsf11b | 18383 | tumor necrosis factor receptor superfamily, member 11b (osteoprotegerin) | 1.38505666 | 2.25E-282 yes | |
| 50 | Efemp1 | 216616 | epidermal growth factor-containing fibulin-like extracellular matrix protein 1 | 1.3816252 | 0 yes | |
| 51 | Ank3 | 11735 | ankyrin 3, epithelial | 1.37355897 | 0 | |
| 52 | Slmap | 83997 | sarcomlemma associated protein | 1.34483371 | 0 | |
| 53 | Jun | 16476 | jun proto-oncogene | 1.33738583 | 0 | |
| 54 | Marcks1 | 17357 | MARCKS-like 1 | 1.3316062 | 0 | |
| 55 | Epas1 | 13819 | endothelial PAS domain protein 1 | 1.32286116 | 0 | |
| 56 | ler2 | 15936 | immediate early response 2 | 1.30297403 | 1.00E-275 | |
| 57 | Cks2 | 66197 | CDC28 protein kinase regulatory subunit 2 | 1.25692235 | 0 | |
| 58 | Egr1 | 13653 | early growth response 1 | 1.24599149 | 1.84E-238 | |
| 59 | Sema6d | 214968 | sema domain, transmembrane domain (TM), and cytoplasmic domain, (semaphorin) 6D | 1.24510045 | 0 | |
| 60 | Ly6e | 17069 | lymphocyte antigen 6 complex, locus E | 1.24406997 | 0 | |
| 61 | H2-K1 | 14972 | histocompatibility 2, K1, region | 1.23087871 | 0 | |
| 62 | Cebpd | 12609 | CCAAT/enhancer binding protein (CEBP), delta | 1.22509248 | 9.65E-304 | |
| 63 | AW112010 | 107350 | expressed sequence AW112010 | 1.22490041 | 0 | |
| 64 | Calcr1 | 54598 | calcitonone receptor-like | 1.20911871 | 3.83E-285 | |
| 65 | Tmem141 | 51875 | transmembrane protein 141 | 1.19909844 | 0 | |
| 66 | Cxcl1 | 14825 | chemokine (C-X-C motif) ligand 1 | 1.1974646 | 2.06E-104 | yes |
| 67 | Aldh2 | 11669 | aldehyde dehydrogenase 2, mitochondrial | 1.19428768 | 0 | |
| 68 | Fos | 14281 | FBX osteosarcoma oncogene | 1.17440579 | 3.30E-266 | |
| 69 | Tmem47 | 192216 | transmembrane protein 47 | 1.16047924 | 0 | |
| 70 | Btg2 | 12227 | BTG anti-proliferation factor 2 | 1.14895829 | 1.68E-214 | |
| 71 | Ednrb | 13617 | endothelin receptor type A | 1.12404858 | 0 | |
| 72 | Cd151 | 12476 | CD151 antigen | 1.11404397 | 0 | |
| 73 | Cadm3 | 94332 | cell adhesion molecule 3 | 1.11336374 | 0 | |
| 74 | Crip2 | 68337 | cysteine rich protein 2 | 1.08824455 | 0 | |
| 75 | Rbm46 | 633285 | RNA binding motif protein 46 | 1.08685319 | 1.61E-66 | |
| 76 | Lgals3bp | 19039 | lectin, galectoside-binding, soluble, 3 binding protein | 1.08353448 | 0 yes | |
| 77 | Fhi1 | 14198 | four and a half LIM domains 1 | 1.06602771 | 1.64E-276 | |
| 78 | Ntm | 235108 | neurotrinin | 1.0612186 | 0 | |
| 79 | Ngfr | 18053 | nerve growth factor receptor (TNFR superfamily, member 16) | 1.03522888 | 3.53E-197 | |
| 80 | Ifitm3 | 66141 | interferon induced transmembrane protein 3 | 1.03163125 | 0 | |
| 81 | B2m | 12010 | beta-2 microglobulin | 1.02913423 | 0 yes | |
| 82 | Nrlf4 | 20186 | nuclear receptor subfamily 1, group H, member 4 | 1.02723652 | 9.22E-271 | |
| 83 | Adra2b | 11552 | adrenergic receptor, alpha 2B | 1.02250967 | 9.95E-280 | |
| 84 | Tnfrsf21 | 94185 | tumor necrosis factor receptor superfamily, member 21 | 1.01818063 | 1.48E-268 | |
| 85 | Ms44d | 66607 | membrane-spanning 4-domains, subfamily A, member 4D | 1.01613591 | 5.16E-272 | |
| 86 | Apold1 | 381823 | apolipoprotein L domain containing 1 | 1.015522 | 5.92E-246 | |
| 87 | Junb | 16477 | jun B proto-oncogene | 1.01321144 | 1.37E-266 | |
| 88 | Sorbs1 | 20411 | sorbin and SH3 domain containing 1 | 0.99987005 | 2.19E-302 | |
| 89 | Icam1 | 15894 | intercellular adhesion molecule 1 | 0.98264274 | 1.81E-178 | |
| 90 | Zeb2 | 24136 | zinc finger E-box binding homeobox 2 | 0.97100654 | 0 | |
| 91 | Bmp10 | 12154 | bone morphogenetic protein 10 | 0.96504463 | 3.78E-306 | yes |
| 92 | Cfb | 14962 | complement factor B | 0.96478453 | 5.61E-226 | yes |
| 93 | Ets1 | 23871 | E26 avian leukemia oncogene, 1, 5' domain | 0.96438055 | 8.40E-258 | |
| 94 | Nfkbia | 18035 | nuclear factor of kappa light polypeptide gene enhancer in B cells inhibitor, alpha | 0.96160691 | 5.47E-159 | |
| 95 | Phlda1 | 21664 | pleckstrin homology like domain, family A, member 1 | 0.95632866 | 1.19E-187 | |
| 96 | Adm | 11535 | adrenomedullin | 0.94876781 | 4.95E-186 | yes |
| 97 | Ifna2 | 15976 | interferon (alpha and beta) receptor 2 | 0.94206898 | 0 yes | |
| 98 | Isg15 | 100038882 | ISG15 ubiquitin-like modifier | 0.93535458 | 5.94E-131 | yes |
| 99 | Ifi3 | 15959 | interferon-induced protein with tetratricopeptide repeats 3 | 0.92884293 | 4.40E-207 | |
| 100 | Lhx2 | 16870 | LIM homeobox protein 2 | 0.92734425 | 3.42E-196 | |
| 101 | Tinag1 | 94242 | tubulointerstitial nephritis antigen-like 1 | 0.89098935 | 4.01E-188 | yes |
| 102 | Lama1 | 16772 | laminin, alpha 1 | 0.89055316 | 3.71E-214 | yes |
| 103 | Ptf4 | 56744 | platelet factor 4 | 0.89012931 | 1.47E-182 | yes |
| 104 | Bco1 | 63857 | beta-carotene oxygenase 1 | 0.88698383 | 6.04E-233 | |
| 105 | Ngf | 18049 | nerve growth factor | 0.88209514 | 2.13E-177 | yes |
| 106 | Apoe | 11816 | apolipoprotein E | 0.87559721 | 2.97E-254 | yes |
| 107 | Arhgap42 | 71544 | Rho GTPase activating protein 42 | 0.87414577 | 9.16E-220 | |

| | | | | | |
|-----|----------|-----------|---|------------|-----------|
| 108 | Ephx1 | 13849 | epoxide hydrolase 1, microsomal | 0.85948655 | 1.19E-226 |
| 109 | Papss2 | 23972 | 3'-phosphoadenosine 5'-phosphosulfate synthase 2 | 0.83553512 | 1.25E-201 |
| 110 | Tshz2 | 228911 | (teashirt zinc finger family member 2 | 0.83380001 | 2.70E-221 |
| 111 | Rarres2 | 71660 | retinoic acid receptor responder (tazarotene induced) 2 | 0.83364757 | 0 yes |
| 112 | Smagp | 207818 | small cell adhesion glycoprotein | 0.83184116 | 1.74E-272 |
| 113 | Arap2 | 212285 | ArfGAP with RhoGAP domain, ankyrin repeat and PH domain 2 | 0.82809673 | 3.53E-190 |
| 114 | Trp53i11 | 277414 | transformation related protein 53 inducible protein 11 | 0.82802883 | 1.95E-229 |
| 115 | Bcr | 110279 | BCR activator of RhoGEF and GTPase | 0.82213242 | 1.86E-125 |
| 116 | Eps8 | 13860 | epidermal growth factor receptor pathway substrate 8 | 0.80425612 | 3.82E-191 |
| 117 | P2ry14 | 140795 | purinergic receptor P2Y ₁₄ , G-protein coupled, 14 | 0.79913764 | 1.10E-168 |
| 118 | Sifn5 | 327978 | schlafen 5 | 0.79703 | 2.58E-185 |
| 119 | H2-Q4 | 15015 | histocompatibility 2, Q region locus 4 | 0.77195543 | 3.30E-164 |
| 120 | Gm14964 | 100008567 | predicted gene 14964 | 0.75002718 | 1.46E-183 |
| 121 | Spry1 | 24063 | sprouty RTK signalling antagonist 1 | 0.7407657 | 4.42E-167 |
| 122 | Bst2 | 69550 | bone marrow stromal cell antigen 2 | 0.73333396 | 1.48E-192 |
| 123 | Klin1 | 16709 | kinectin 1 | 0.71946095 | 7.94E-145 |
| 124 | Gqt5 | 23887 | gamma-glutamyltransferase 5 | 0.63971252 | 3.24E-164 |
| 125 | Cyp20a1 | 77951 | cytochrome P450, family 20, subfamily a, polypeptide 1 | 0.55212791 | 1.20E-93 |

Supplementary Table 4. GO biological process enrichment pathway analysis showing the top biological processes for mouse myHSC (a) and cyHSC (b) signatures.
 adj_p.value: adjusted p.value.

a. myHSC

| Pathways | Genes (n)/ all genes (n) | p.value | adj_p.value |
|---|--------------------------|-------------|-------------|
| Extracellular matrix organization (GO:0030198) | 30/359 | 3.14827E-30 | 2.65902E-27 |
| Extracellular structure organization (GO:0043062) | 30/360 | 3.42436E-30 | 2.65902E-27 |
| Extracellular matrix disassembly (GO:0022617) | 17/116 | 1.85033E-21 | 9.57854E-19 |
| Collagen metabolic process (GO:0032963) | 14/83 | 9.98718E-19 | 3.87752E-16 |
| Collagen catabolic process (GO:0030574) | 13/74 | 1.05378E-17 | 2.33789E-15 |
| Response to wounding (GO:0009611) | 11/167 | 2.32479E-10 | 3.6104E-08 |
| Collagen fibril organization (GO:0030199) | 7/41 | 5.84916E-10 | 8.25795E-08 |
| Response to transforming growth factor beta (GO:0071559) | 9/166 | 5.97468E-08 | 6.62762E-06 |
| Cellular response to transforming growth factor beta stimulus (GO:0071560) | 9/166 | 5.97468E-08 | 6.62762E-06 |
| Regulation of transforming growth factor beta receptor signaling pathway (GO:0017015) | 7/103 | 4.11506E-07 | 3.04318E-05 |
| Wound healing (GO:0042060) | 6/75 | 1.10064E-06 | 6.33072E-05 |

b. cyHSC

| Pathways | Genes (n)/ all genes (n) | p.value | adj_p.value |
|---|--------------------------|--------------|-------------|
| Response to lipopolysaccharide (GO:0032496) | 13/228 | 1.93621E-09 | 1.26693E-06 |
| Negative regulation of locomotion (GO:0040913) | 12/204 | 5.89365E-09 | 2.31385E-06 |
| Negative regulation of cell migration (GO:0030336) | 11/166 | 7.56968E-09 | 2.47655E-06 |
| Negative regulation of cell motility (GO:2000146) | 11/170 | 9.71062E-09 | 2.72314E-06 |
| Response to interferon-alpha (GO:0035455) | 5/17 | 5.12656E-08 | 1.11816E-05 |
| Regulation of leukocyte migration (GO:002685) | 8/110 | 4.46692E-07 | 7.97142E-05 |
| Cellular response to cytokine stimulus (GO:0071345) | 14/471 | 1.50236E-06 | 0.00024326 |
| Cytokine-mediated signaling pathway (GO:0019221) | 12/342 | 0.0000016111 | 0.00024326 |
| Response to hypoxia (GO:0001666) | 10/241 | 2.8283E-06 | 0.00037822 |
| Cellular response to type I interferon (GO:0071357) | 6/65 | 3.22734E-06 | 0.00037822 |
| Type I interferon signaling pathway (GO:0060337) | 6/65 | 3.22734E-06 | 0.00037822 |
| Response to type I interferon (GO:0034340) | 6/66 | 3.53204E-06 | 0.000385189 |
| Regulation of epithelial cell proliferation (GO:0050678) | 10/258 | 5.18027E-06 | 0.000501047 |
| Positive regulation of leukocyte migration (GO:0002687) | 6/78 | 9.3931E-06 | 0.000801681 |
| Negative regulation of immune system process (GO:0002683) | 10/311 | 2.62064E-05 | 0.001599118 |
| Response to extracellular stimulus (GO:0009991) | 10/313 | 2.76763E-05 | 0.001599118 |
| Regulation of mononuclear cell migration (GO:0071675) | 3/10 | 2.76974E-05 | 0.001599118 |
| Transmembrane receptor protein serine/threonine kinase signaling pathway (GO:0007178) | 8/196 | 3.25955E-05 | 0.00178901 |
| Regeneration (GO:0031099) | 6/97 | 3.28092E-05 | 0.00178901 |
| Defense response to virus (GO:0051607) | 7/147 | 3.88386E-05 | 0.002060545 |
| Positive regulation of endothelial cell proliferation (GO:0001938) | 5/63 | 4.62801E-05 | 0.002390731 |
| Regulation of myeloid cell differentiation (GO:0045637) | 7/156 | 5.66884E-05 | 0.002800532 |
| Response to alcohol (GO:0097305) | 9/274 | 5.70664E-05 | 0.002800532 |
| Response to interferon-gamma (GO:0034341) | 6/108 | 6.00806E-05 | 0.002876544 |
| Regulation of cAMP metabolic process (GO:0030814) | 6/113 | 7.73391E-05 | 0.003469888 |
| Response to interleukin-1 (GO:0070555) | 5/71 | 8.23786E-05 | 0.003504465 |
| Extracellular matrix organization (GO:0030198) | 10/359 | 8.72365E-05 | 0.003604465 |
| Positive regulation of cAMP metabolic process (GO:0030816) | 5/72 | 8.80867E-05 | 0.003504465 |
| Extracellular structure organization (GO:0043062) | 10/360 | 8.93621E-05 | 0.003504465 |

Supplementary Table 5. Top 25 genes encoding secreted proteins in myHSC (a) and cyHSC (b) subpopulations, determined by the signatures generated in Supplementary Information.3. avg_log2FC: average log2 fold change; adj_p.value: adjusted p.value.

a. TOP 25 myHSC GENES ENCODING

| Gene_name | avg_log2FC | adj_p_value |
|---------------|-------------|-------------|
| Spp1 | 4.11 | 0 |
| Mgp | 3.63 | 0 |
| Timp1 | 3.02 | 0 |
| Serpine2 | 3.01 | 0 |
| Ptn | 2.48 | 0 |
| Col15a1 | 2.45 | 0 |
| Col1a1 | 2.45 | 0 |
| Eln | 2.43 | 0 |
| Lpl | 2.38 | 0 |
| Ltbp2 | 2.1 | 0 |
| Dpt | 1.96 | 0 |
| Col1a2 | 1.89 | 0 |
| Lgals1 | 1.83 | 0 |
| Serpina3n | 1.82 | 0 |
| Mfap4 | 1.79 | 0 |
| Sparcl1 | 1.73 | 0 |
| Htra1 | 1.69 | 0 |
| Fbn2 | 1.67 | 0 |
| Tnc | 1.59 | 0 |
| Timp3 | 1.58 | 0 |
| Plat | 1.57 | 0 |
| Col6a3 | 1.53 | 0 |
| Igf1 | 1.49 | 0 |
| Lox11 | 1.46 | 0 |
| Ncam1 | 1.44 | 0 |

b. TOP 25 cyHSC GENES ENCODING

| Gene_name | avg_log2FC | adj_p_value |
|------------|-------------|-------------|
| Colec11 | 3.48 | 0 |
| Angptl6 | 3.19 | 0 |
| Ecm1 | 2.88 | 0 |
| Fcna | 2.58 | 0 |
| Colec10 | 2.5 | 0 |
| Rein | 2.5 | 0 |
| Masp1 | 2.28 | 0 |
| Cxcl12 | 2.25 | 0 |
| Sod3 | 2.22 | 0 |
| Col14a1 | 2.19 | 0 |
| Gdf2 | 2.16 | 0 |
| Dcn | 2.13 | 0 |
| Igfbp3 | 2.02 | 0 |
| Wfdc1 | 1.99 | 0 |
| Tgfb1 | 1.98 | 0 |
| Rspo3 | 1.89 | 0 |
| Ccl2 | 1.69 | 6.88E-162 |
| Hgf | 1.64 | 0 |
| Prelp | 1.63 | 0 |
| Bmp5 | 1.39 | 0 |
| Tnfrsf11b | 1.39 | 2.25E-282 |
| Efemp1 | 1.38 | 0 |
| Cxcl1 | 1.2 | 2.06E-104 |
| Lgals3bp | 1.08 | 0 |
| B2m | 1.03 | 0 |

Supplementary Table 6. cyHSC (a) and myHSC (b) genes used to determine cyHSC-myHSC balance in patient cohorts. The Avg_logFC: log fold-change of the average expression between highly and less activated HSC. Positive values indicate that the genes are more highly expressed in the highly activated HSC, negative values indicate that the genes are highly expressed in the less activated HSC. p_val_adj : adjusted p-value.

a. cyHSC genes for dysbalance

| Gene name | Gene ID | Description | avg_logFC | p_val_adj | Secreted |
|-----------|-----------|---|-------------|-----------|----------|
| Colec11 | 71693 | collectin sub-family member 11 | 3.484632549 | 0 | yes |
| Angptl6 | 70726 | angiotropin-like 6 | 3.189066616 | 0 | yes |
| Ecm1 | 13601 | extracellular matrix protein 1 | 2.879760264 | 0 | yes |
| Fcna | 14133 | ficolin A | 2.583451534 | 0 | yes |
| Colec10 | 239447 | collectin subfamily member 10 | 2.500584448 | 0 | yes |
| Reln | 19699 | reelin | 2.495826867 | 0 | yes |
| Masp1 | 17174 | MBL associated serine protease 1 | 2.279544496 | 0 | yes |
| Cxcl12 | 20315 | C-X-C motif chemokine ligand 12 | 2.246027603 | 0 | yes |
| Sod3 | 20657 | superoxide dismutase 3 | 2.216992137 | 0 | yes |
| Col14a1 | 12818 | collagen type XIV alpha 1 chain | 2.188322344 | 0 | yes |
| Gdf2 | 12165 | growth differentiation factor 2 | 2.156964409 | 0 | yes |
| Dcn | 13179 | decorin | 2.132717575 | 0 | yes |
| Igfbp3 | 16009 | insulin-like growth factor binding protein 3 | 2.017296308 | 0 | yes |
| Wfdc1 | 67866 | WAP four-disulfide core domain 1 | 1.989478799 | 0 | yes |
| Tgfb1 | 21810 | transforming growth factor, beta induced | 1.978309057 | 0 | yes |
| Rspo3 | 72780 | R-spondin 3 | 1.889292553 | 0 | yes |
| Ccl2 | 20296 | C-C motif chemokine ligand 2 | 1.687787428 | 6.88E-162 | yes |
| Hgf | 15234 | hepatocyte growth factor | 1.640505773 | 0 | yes |
| Prelp | 116847 | proline and arginine rich end leucine rich repeat protein | 1.630229311 | 0 | yes |
| Bmp5 | 12160 | bone morphogenetic protein 5 | 1.394146042 | 0 | yes |
| Tnfrsf11b | 18383 | TNF receptor superfamily member 11B | 1.385056655 | 2.25E-282 | yes |
| Efemp1 | 216616 | EGF containing fibulin extracellular matrix protein 1 | 1.381625204 | 0 | yes |
| Cxcl1 | 14825 | C-X-C motif chemokine ligand 1 | 1.197464597 | 2.06E-104 | yes |
| Lgals3bp | 19039 | galectin 3 binding protein | 1.08335448 | 0 | yes |
| B2m | 12010 | beta-2 microglobulin | 1.029134235 | 0 | yes |
| Bmp10 | 12154 | bone morphogenetic protein 10 | 0.965044632 | 3.78E-306 | yes |
| Ctb | 14962 | complement factor B | 0.964784529 | 5.61E-226 | yes |
| Adm | 11535 | adrenomedullin | 0.948767809 | 4.95E-186 | yes |
| Ifnar2 | 5976 | interferon alpha and beta receptor subunit 2 | 0.942068975 | 0 | yes |
| Isgr1 | 100038882 | ISG15 ubiquitin-like modifier | 0.935354584 | 5.94E-131 | yes |
| Tinag1 | 94424 | tubulointerstitial nephritis antigen-like 1 | 0.890989346 | 4.01E-188 | yes |
| Lama1 | 16772 | laminin subunit alpha 1 | 0.890553157 | 3.71E-214 | yes |
| Pf4 | 56744 | platelet factor 4 | 0.890129312 | 1.47E-182 | yes |
| Ngf | 18049 | nerve growth factor | 0.882095143 | 2.13E-177 | yes |
| Apoe | 11816 | apolipoprotein E | 0.875597211 | 2.97E-254 | yes |
| Rarres2 | 71660 | retinoic acid receptor responder 2 | 0.833647565 | 0 | yes |

b. myHSC genes for dysbalance

| Gene name | Gene ID | Description | avg_logFC | p_val_adj | Secreted |
|-----------|---------|--|--------------|-----------|----------|
| Spp1 | 20750 | secreted phosphoprotein 1 | 4.114145131 | 0 | yes |
| Mgp | 17313 | matrix Gla protein | 3.628214502 | 0 | yes |
| Timp1 | 21857 | TIMP metallopeptidase inhibitor 1 | 3.02414586 | 0 | yes |
| Serpine2 | 20720 | serpin family E member 2 | 3.010402684 | 0 | yes |
| Ptn | 19242 | pleiotrophin | 2.484395056 | 0 | yes |
| Col15a1 | 12819 | collagen type XV alpha 1 chain | 2.449939885 | 0 | yes |
| Col1a1 | 12842 | collagen type I alpha 1 chain | 2.447026237 | 0 | yes |
| Eln | 13717 | elastin | 2.426745974 | 0 | yes |
| Lpl | 16956 | lipoprotein lipase | 2.380721258 | 0 | yes |
| Ltbp2 | 16997 | latent transforming growth factor beta binding protein 2 | 2.103696756 | 0 | yes |
| Dpt | 56429 | dermatopontin | 1.95931805 | 0 | yes |
| Col1a2 | 12843 | collagen type I alpha 2 chain | 1.894798899 | 0 | yes |
| Lgals1 | 16852 | galectin 1 | 1.831543817 | 0 | yes |
| Serpina3n | 20716 | serpin family A member 3 | 1.819086561 | 0 | yes |
| Mfap4 | 76293 | microfibril associated protein 4 | 1.787033453 | 0 | yes |
| Spard1 | 13602 | SPARC like 1 | 1.731738413 | 0 | yes |
| Htr1a | 56213 | HtrA serine peptidase 1 | 1.685952809 | 0 | yes |
| Fbn2 | 14119 | fibrillin 2 | 1.673157506 | 0 | yes |
| Tnc | 21923 | tenascin C | 1.59174016 | 0 | yes |
| Timp3 | 21859 | TIMP metallopeptidase inhibitor 3 | 1.575243024 | 0 | yes |
| Plat | 18791 | plasminogen activator, tissue type | 1.572147289 | 0 | yes |
| Col6a3 | 12835 | collagen type VI alpha 3 chain | 1.528521617 | 0 | yes |
| Igf1 | 16000 | insulin like growth factor 1 | 1.494235809 | 0 | yes |
| Lox1 | 16949 | lysyl oxidase like 1 | 1.458796533 | 0 | yes |
| Ncam1 | 17967 | neural cell adhesion molecule 1 | 1.439169518 | 0 | yes |
| Gas6 | 14456 | growth arrest specific 6 | 1.365753972 | 0 | yes |
| Col8a1 | 12837 | collagen type VIII alpha 1 chain | 1.318605635 | 5.73E-287 | yes |
| Col5a2 | 12832 | collagen type V alpha 2 chain | 1.294930587 | 0 | yes |
| Lox | 16948 | lysyl oxidase | 1.265524707 | 0 | yes |
| Col4a5 | 12830 | collagen type IV alpha 5 chain | 1.202458835 | 0 | yes |
| Cxcl14 | 57266 | (C-X-C motif) chemokine ligand 14 | 1.189068683 | 4.61E-112 | yes |
| Mfap2 | 17150 | microfibril associated protein 2 | 1.177496807 | 0 | yes |
| Col3a1 | 12825 | collagen type III alpha 1 chain | 1.176094148 | 0 | yes |
| Fstl1 | 14314 | follistatin like 1 | 1.157727505 | 0 | yes |
| Mdk | 17242 | midkine | 1.092427577 | 2.47E-260 | yes |
| Fam180a | 208164 | family with sequence similarity 180 member A | 1.088779238 | 0 | yes |
| Pdgfr | 68797 | platelet derived growth factor receptor like | 1.071376115 | 0 | yes |
| Aebp1 | 11568 | AE binding protein 1 | 1.0588994876 | 0 | yes |
| Col6a2 | 12834 | collagen type VI alpha 2 chain | 1.049962532 | 0 | yes |
| Pla1a | 85031 | phospholipase A1 member A | 1.0457689 | 0 | yes |
| Crispld2 | 78892 | cysteine rich secretory protein LCL domain containing 2 | 1.04445127 | 1.01E-261 | yes |
| Igfbp4 | 16010 | insulin like growth factor binding protein 4 | 1.035744403 | 5.66E-144 | yes |
| Mmp2 | 17390 | matrix metalloproteinase 2 | 1.007010061 | 6.98E-212 | yes |

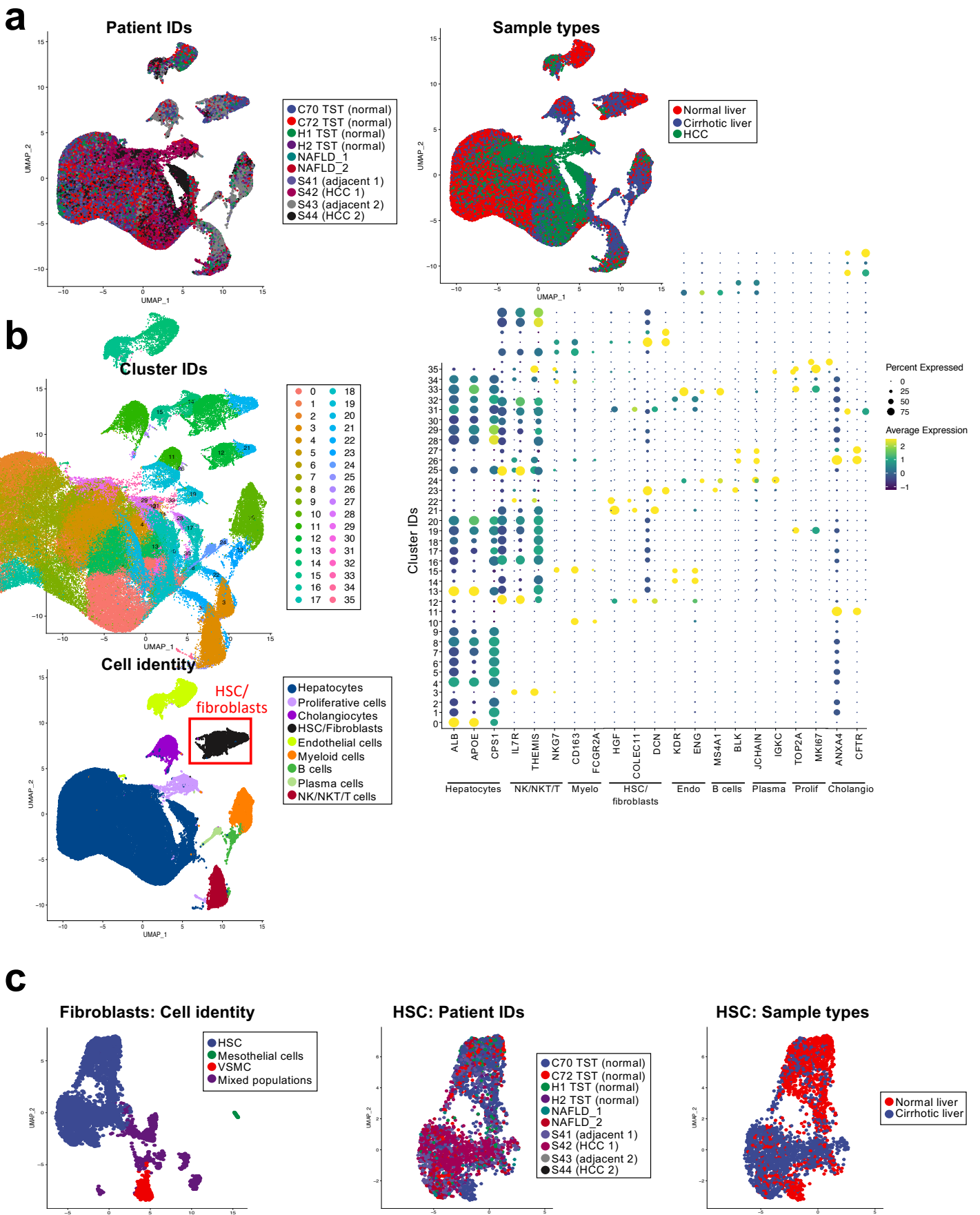
Supplementary Table 7: Summary of all mouse HCC models used in this study. LBR: liver/body weight ration, ND: not determined

| Figure in manuscript | Strain | HCC Model | Effect on liver cell populations | Effect of genetic alteration on HCC development | n per group | LBR (%) | | | Tumour number (n) | | | Tumor size (mm) | | |
|----------------------|------------------------------------|--|--|---|----------------------|----------------------------------|--------------------------------------|--------------------------------------|----------------------------------|----------------------------------|----------------------------------|----------------------------------|----------------------------------|--------------------------------------|
| | | | | | | Mean | SD | SEM | Mean | SD | SEM | Mean | SD | SEM |
| Fig. 1b | Lhx2 <i>fl/fl</i> Lhx2ΔHSC | DEN | HSC activation | increases HCC | 8 7 | 7.762 12.29 | 3.368 2.926 | 1.191 1.106 | 43.63 64.57 | 18.56 8.696 | 6.563 3.287 | 6.893 11.71 | 2.918 1.691 | 1.032 0.6392 |
| Ext.Fig. 2f | Lhx2 <i>fl/fl</i> Lhx2 del | DEN | HSC activation | increases HCC | 11 9 | 5.772 11.37 | 2.398 4.205 | 0.723 1.402 | 3 14.11 | 2.49 4.885 | 0.751 1.628 | 4.227 12.78 | 3.663 4.309 | 1.104 1.436 |
| Fig. 1d | YAP <i>fl/fl</i> YAP AHSC | DEN+14xCCI4 (1xCCI4 per week) | HSC inhibition | reduces HCC | 15 16 15 17 | 7.735 6.492 6.284 5.099 | 1.489 0.8877 0.8633 0.6254 | 0.3845 0.2219 0.2229 0.1517 | 88 58.88 84.33 63.88 | 28.33 25.25 27.5 25.53 | 7.315 3.366 4.247 3.404 | 5.301 1.976 8.536 7.433 | 2.069 1.796 8.536 1.803 | 0.5529 0.494 2.204 1.803 |
| Fig. 1f | DTRneg DTRpos | DEN+14xCCI4 (DT: late depletion) | depletion of HSC | reduces HCC | 15 16 17 18 | 6.284 6.099 5.999 6.151 | 0.8633 0.8633 0.6254 0.8223 | 0.2229 0.2229 0.1517 0.1517 | 84.33 63.88 63.88 63.88 | 27.5 25.53 25.53 25.53 | 7.101 6.193 6.193 6.193 | 4.247 3.404 3.404 3.404 | 8.536 7.433 7.433 7.433 | 2.204 1.803 1.803 1.803 |
| Ext.Fig. 2g | aSMAneg aSMAnpos | DEN+17xCCI4 (GCV: late depletion) | depletion of aSMA+ cells | reduces HCC | 13 13 13 13 | 8.151 6.608 6.608 6.608 | 1.882 0.9469 0.9469 0.9469 | 0.5219 0.4969 0.4969 0.4969 | 106.2 90.08 90.08 90.08 | 24.45 24.45 24.45 24.45 | 6.78 6.78 6.78 6.78 | 7.062 6.062 6.062 6.062 | 1.334 0.963 0.963 0.963 | 0.3699 0.2672 0.2672 0.2672 |
| Ext.Fig. 2m | Pdgfrb <i>fl/fl</i> Pdgfrb ΔHSC | Mdr2KO 15m | HSC inhibition | reduces HCC | 8 6 | 11.26 7.809 | 4.183 1.521 | 1.479 0.6211 | 59.38 31.17 | 31.12 17.95 | 11 7.328 | 8.824 7.578 | 3.246 1.958 | 1.148 0.7994 |
| Ext.Fig. 2p | DTRneg DTRpos | TAZ+NPC | depletion of HSC | reduces HCC | 10 14 | 10.44 7.044 | 3.179 1.017 | 1.005 0.2719 | 11.6 5.286 | 9.046 4.514 | 2.86 1.206 | 6.78 4.657 | 3.03 1.526 | 0.9581 0.4079 |
| Ext.Fig. 2r | DTRneg DTRpos | DEN+HF-CDAA (DT: late depletion) | depletion of HSC | reduces HCC | 6 8 | 10.02 6.479 | 0.6023 0.618 | 0.2459 0.2185 | 19 4.125 | 9.92 3.441 | 4.05 1.217 | 4.922 3.667 | 1.013 1.523 | 0.4136 0.5383 |
| Ext.Fig. 2u | aSMAneg aSMAnpos | NICD1+CDAA (GCV: late depletion) | depletion of aSMA+ cells | reduces HCC | 9 8 | 10.11 9.824 | 0.7535 0.7986 | 0.2512 0.2823 | 2.222 0.875 | 1.202 1.808 | 0.401 0.639 | 3.615 2.313 | 0.496 0.862 | 0.1652 0.3048 |
| Ext.Fig. 4a | aSMAneg aSMAnpos | DEN+CC4 (GCV: late depletion when tumors are formed) | depletion of SMA+ cells in tumours via GCV | no effect observed | 12 10 | 1.054 0.6227 | 0.3635 0.2481 | 0.1021 0.0785 | 3.036 2.418 | 1.963 1.154 | 0.645 0.385 | 10.28 5.945 | 6.626 5.37 | 1.84 1.619 |
| Ext.Fig. 4d | DTRneg DTRpos | MET+CTNBB1 | depletion of HSC | no effect observed | 11 7 | 11.15 11.62 | 5.302 4.113 | 1.599 1.555 | 24.45 22.29 | 15.61 12.11 | 4.707 4.576 | 6.455 5.924 | 5.474 4.713 | 1.65 1.782 |
| Ext.Fig. 7b | DTRneg DTRpos | DEN+14xCCI4 (DT: early depletion) | depletion of HSC | no effect observed | 10 10 | 6.842 6.307 | 0.5651 1.468 | 0.1787 0.4642 | 85 45 | 31.51 14.23 | 9.965 4.607 | 5.28 1.628 | 0.642 0.5148 | 0.203 0.5148 |
| Ext.Fig. 7c | Lhx2 <i>fl/fl</i> Lhx2del | DEN (early time point) | HSC activation | no effect observed | 9 10 | 4.161 6.828 | 0.276 3.231 | 0.098 1.022 | 2.222 12.2 | 1.22 3.858 | 7.768 5.9 | 3.422 4.427 | 1.394 1.4648 | 0.2561 0.4648 |
| Ext.Fig. 7d | Lhx2 <i>fl/fl</i> Lhx2del | DEN (late depletion of Lhx2) | HSC activation | increases HCC | 12 11 | 11.94 11.15 | 5.719 5.302 | 1.651 1.599 | 29.17 24.45 | 14.9 15.61 | 4.303 4.707 | 11.79 6.455 | 5.867 5.474 | 1.694 1.65 |
| Ext.Fig. 1d | Trp53 <i>fl/fl</i> Trp53ΔHSC | DEN+14xCCI4 (1xCCI4 per week) | no effect observed of fibrosis and HSC activation | no effect observed | 14 14 | 6.759 6.759 | 0.7739 0.7739 | 0.2447 0.2447 | 82.64 82.64 | 25.18 25.18 | 7.591 7.591 | 5.188 5.188 | 0.547 0.547 | 0.1648 0.1648 |
| Ext.Fig. 1h | RelA <i>fl/fl</i> RelAΔHSC | DEN+17xCCI4 (1xCCI4 per week) | no effect observed of fibrosis and HSC activation | no effect observed | 9 10 | 6.082 6.07 | 0.4116 0.6725 | 0.1372 0.2127 | 55 55 | 41.62 31.26 | 13.87 9.884 | 3.426 3.42 | 0.501 1.11 | 0.167 0.3511 |
| Ext.Fig. 8d | Col1a1 floxed Col1a1 deleted | DEN+15xCO4 (1xCCI4 per week) | not determined | no effect observed | 17 14 | 7.351 8.012 | 1.303 1.788 | 0.316 0.4779 | 68.24 84.64 | 27.69 28.73 | 6.716 7.679 | 5.047 5.6 | 1.542 1.521 | 0.374 0.4064 |
| Fig. 4a | Col1a1 floxed Col1a1 deleted | DEN+44xCCI4 (profound fibrosis) | Reduced TAZ activation in hepatocytes, hepatocyte proliferation and tumour proliferation | reduces HCC | 21 21 | 8.781 6.79 | 3.398 0.9952 | 0.7416 0.2172 | 12.57 8.667 | 8.536 6.923 | 1.863 1.511 | 7.488 5.533 | 2.597 1.305 | 0.5807 0.2848 |
| Ext.Fig. 8k | Col1a1 floxed Col1a1 deleted | Mdr2KO 15m | not determined | reduces HCC | 18 11 | 9.713 8.697 | 2.518 2.134 | 0.6107 0.6435 | 51.28 22 | 20.58 13.07 | 4.851 3.94 | 6.771 5.508 | 2.528 3.266 | 0.5959 0.9849 |
| Ext.Fig. 8n | Col1a1 floxed Col1a1 AHSC | DEN+44xCCI4 (profound fibrosis) | not determined | reduces HCC | 16 14 | 7.144 6.338 | 1.085 0.7483 | 0.2712 0.2 | 8.375 4.5 | 4.425 3.252 | 1.106 0.869 | 6.185 4.002 | 2.445 0.842 | 0.6113 0.225 |
| Ext.Fig. 8q | Col1a1 floxed Col1a1 AHSC | HF-CDAA-HCC | not determined | reduces HCC | 11 10 | 9.582 9.82 | 0.7225 0.9247 | 0.2178 0.2924 | 4.273 0.8 | 2.37 0.789 | 0.715 2.78 | 5.038 2.387 | 1.359 1.223 | 0.4098 0.1223 |
| Fig. 6a | Hgf <i>fl/fl</i> Hgf ΔHSC | DEN+12xCCI4 (1xCCI4 per week) | Increased hepatocyte death, HSC activation and hepatocyte proliferation | increases HCC | 10 10 | 6.212 6.887 | 0.3344 1.923 | 0.1057 0.6081 | 28.3 122.5 | 21.07 38.73 | 6.662 12.25 | 28.7 61.93 | 5.236 7.406 | 1.656 2.469 |
| Ext.Fig. 11g | Hhip <i>fl/fl</i> Hhip AHSC | DEN | not determined | no effect observed | 17 11 | 6.024 6.545 | 2.741 2.411 | 0.6647 0.7271 | 31.59 30.73 | 27.77 17.22 | 6.736 5.192 | 5.129 5.677 | 2.934 3.188 | 0.7115 0.9614 |
| Ext.Fig. 11l | Cxcl12 <i>fl/fl</i> Cxcl12 ΔHSC | DEN+14xCCI4 (1xCCI4 per week) | not determined | no effect observed | 12 14 | 6.755 6.737 | 1.079 0.6691 | 0.3114 0.1788 | 78 88.29 | 22.67 24 | 6.544 6.415 | 5.567 6.121 | 1.12 1.007 | 0.3232 0.2692 |
| Fig. 4f | Wwt1 <i>fl/fl</i> Wwt1ΔHep | DEN+44xCCI4 (profound fibrosis) | Reduced Hepatocyte proliferation no effect on tumour proliferation | reduces HCC | 10 10 | 6.726 5.618 | 1.149 0.8833 | 0.3634 0.2793 | 15.3 9.1 | 5.458 4.228 | 1.726 1.337 | 6.7 4.4 | 2.247 1.368 | 0.7105 0.4326 |
| Fig. 5c | Ddr1 <i>fl/fl</i> Ddr1 ΔHep | DEN+44xCCI4 (profound fibrosis) | Reduced tumour proliferation | reduces HCC | 10 9 | 6.629 5.625 | 0.792 0.7043 | 0.2505 0.2348 | 12.89 9.444 | 4.372 4.096 | 1.457 1.365 | 7.69 5.87 | 1.434 1.076 | 0.4533 0.3585 |
| Ext.Fig. 9i | Yap1 <i>fl/fl</i> Yap1 ΔHep | DEN+44xCCI4 (profound fibrosis) | ND | no effect observed | 14 10 | 6.578 6.384 | 0.8133 0.7774 | 0.2174 0.2458 | 19.57 23.8 | 8.847 7.772 | 2.364 2.458 | 5 5.1 | 2.051 1.54 | 0.5481 0.487 |
| Ext.Fig. 11d | Has2 <i>fl/fl</i> Has2ΔHSC | DEN+14xCCI4 (1xCCI4 per week) | ND | reduce slightly | 21 20 | 8.197 7.274 | 1.645 1.567 | 0.3589 0.3504 | 111.4 82.4 | 28.85 30.38 | 6.295 6.794 | 5.55 4.915 | 1.022 1.122 | 0.2229 0.2573 |
| Ext.Fig. 9j | Itgb1 <i>fl/fl</i> Itgb1 ΔHep | DEN+44xCCI4 (profound fibrosis) | ND | reduce slightly | 13 11 | 6.231 5.976 | 1.892 1.087 | 0.5249 0.9307 | 25.23 17.36 | 10.08 13.03 | 2.795 3.927 | 7.074 5.652 | 1.621 1.614 | 0.4496 0.4867 |

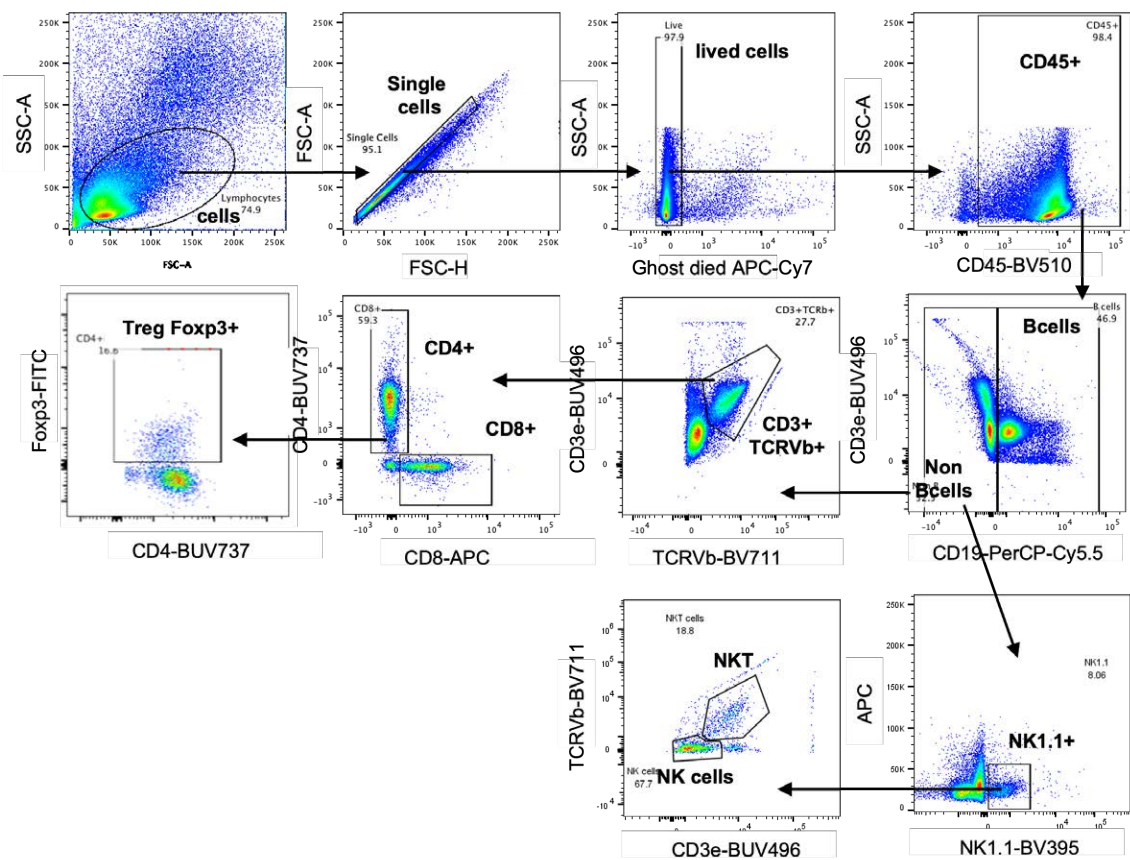
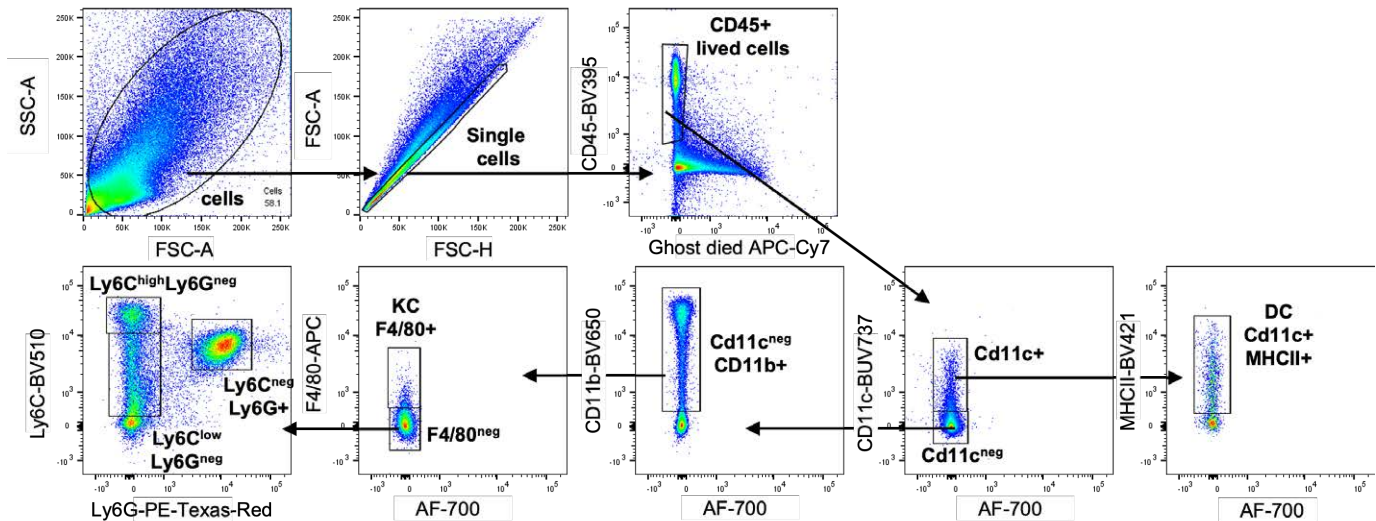
Supplementary Table 8: Summary of proliferation and cell death analysis performed in this study

| Figure in manuscript | Strains | Models | Effect on cell populations | number hepatocyte Ki67+ | | | number tumour cells Ki67+ | | | number hepatocyte TUNEL+ | | |
|-------------------------|---------------------|---|--|-------------------------|-------|-------|---------------------------|-------|-------|--------------------------|-------|-------|
| | | | | Mean | SD | SEM | Mean | SD | SEM | Mean | SD | SEM |
| Fig.2c and Ext.Fig. 3k | YAP <i>ff</i> | DEN+14xCCl4 (quantification determined 2 days after last CCl4 injection) | HSC inhibition does not affect hepatocyte proliferation but reduced hepatocyte death | 64.28 | 33.65 | 10.64 | | | | 84.54 | 45.73 | 11.81 |
| | YAP Δ HSC | | | 56.87 | 13.2 | 3.98 | | | | 40.14 | 27.98 | 6.996 |
| Ext.Fig. 3k-l | aSMAneg | 6xCCl4 (quantification determined 2 days after last CCl4 injection) | deplete aSMA+ cells reduces hepatocyte proliferation and hepatocyte death | 62.4 | 17.08 | 6.039 | ND | ND | ND | 50.78 | 22.64 | 7.161 |
| | aSMApos | | | 31.69 | 12.14 | 6.069 | ND | ND | ND | 9.16 | 3.938 | 1.761 |
| Fig.2c | DTRneg | DEN+14xCCl4 (DT: late depletion) (quantification determined 3 days after last CCl4 injection) | deplete HSC reduces hepatocyte proliferation | 83.01 | 33.17 | 10.49 | | | | ND | ND | ND |
| | DTRpos | | | 38.04 | 21.83 | 6.902 | | | | ND | ND | ND |
| Fig. 6b | Hgf <i>ff</i> | 6xCCl4 (quantification determined 2 days after last CCl4 injection) | HGF deletion in HSC increases liver injury, and hepatocyte proliferation | 275 | 58.22 | 20.58 | ND | ND | ND | 27.82 | 26.54 | 9.382 |
| | Hgf Δ HSC | | | 462 | 70.69 | 35.35 | ND | ND | ND | 90.22 | 34.35 | 17.17 |
| Fig. 4b and Ext.Fig. 9a | Col1a1 <i>ff</i> | DEN+44xCCl4 (profound fibrosis) | Col1a1 deletion reduces TAZ activation in hepatocytes, hepatocyte proliferation and tumour cells proliferation | 22.91 | 18.19 | 5.046 | 45.81 | 25.47 | 7.679 | 8.267 | 2.522 | 1.03 |
| | Col1a1 deleted | (quantification determined 1 week after last injection of CCl4) | | 9.584 | 5.058 | 1.403 | 24.95 | 13.02 | 4.117 | 9.3 | 3.507 | 1.432 |
| Ext.Fig. 8o | Col1a1 <i>ff</i> | DEN+44xCCl4 (profound fibrosis) | Col1a1 deletion in HSC reduces hepatocyte proliferation and trend to reduce tumour proliferation | 15.42 | 7.752 | 2.15 | 50.71 | 19.26 | 6.421 | ND | ND | ND |
| | Col1a1 Δ HSC | (quantification determined 1 week after last injection of CCl4) | | 9.835 | 6.141 | 1.641 | 35.96 | 17.36 | 5.788 | ND | ND | ND |
| Fig. 4f | Wwtr1 <i>ff</i> | DEN+44xCCl4 (profound fibrosis) | TAZ deletion in hepatocyte reduces Hepatocyte proliferation but not tumor cells proliferation | 16.02 | 6.543 | 2.069 | 46.52 | 24.77 | 7.832 | ND | ND | ND |
| | Wwtr1 Δ Hep | (quantification determined 1 week after last injection of CCl4) | | 10.36 | 4.578 | 1.448 | 55.1 | 26.06 | 9.215 | ND | ND | ND |
| Fig. 5d | Ddr1 <i>ff</i> | DEN+44xCCl4 (profound fibrosis) | DDR1 deletion in hepatocyte reduces tumour proliferation | 26.34 | 18.18 | 6.059 | 78.67 | 41.77 | 13.92 | ND | ND | ND |
| | Ddr1 Δ Hep | (quantification determined 1 week after last injection of CCl4) | | 17.48 | 8.49 | 3.002 | 41.37 | 23.9 | 8.452 | ND | ND | ND |

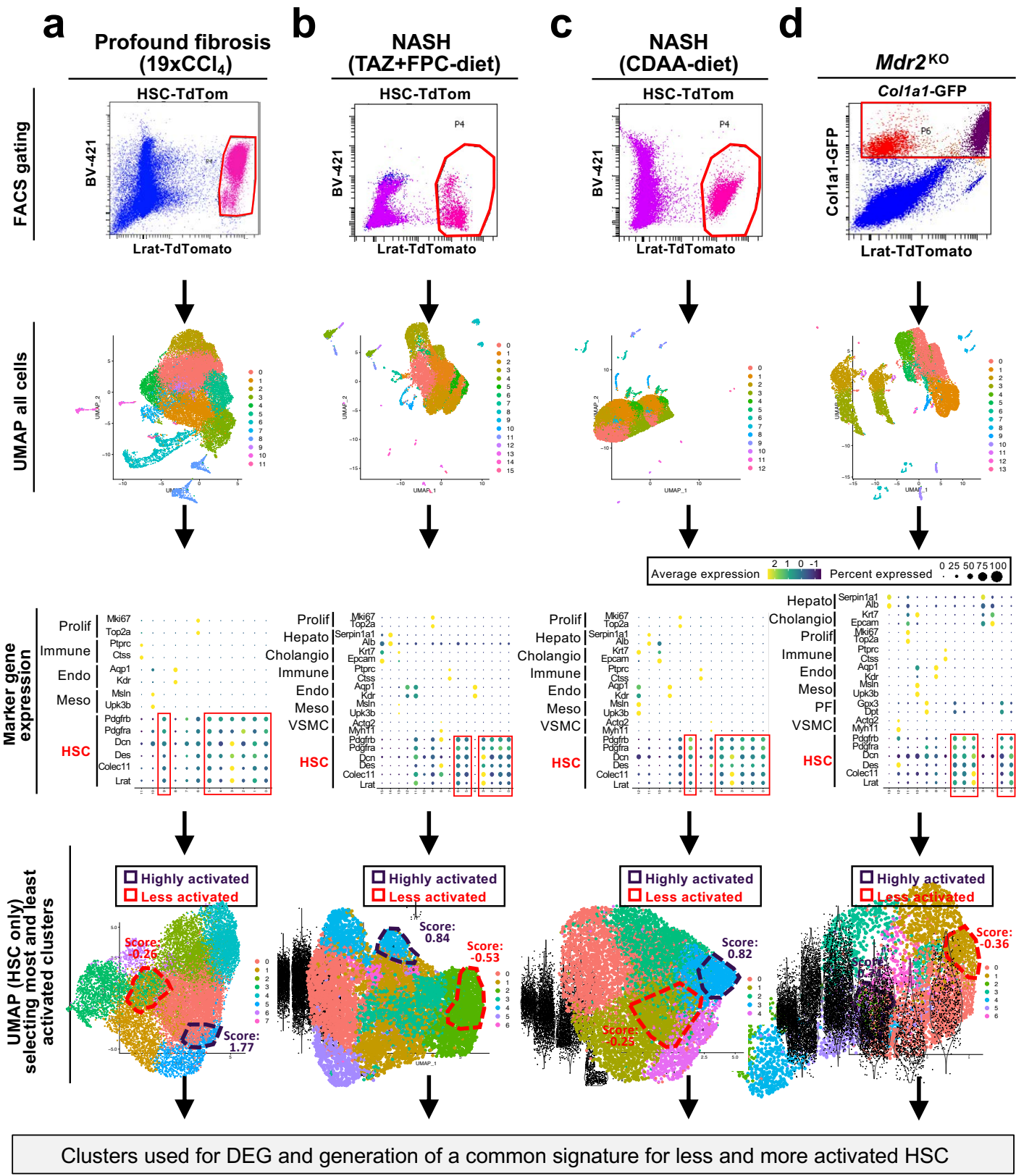
| Figure in manuscript | Strain | Model | Effect on cell populations | tumour Ki67+ area (%) | | |
|----------------------|------------------|---|---|-----------------------|--------|--------|
| | | | | Mean | SD | SEM |
| Ext.Fig. 3m | YAP <i>ff</i> | DEN+14xCCl4 (quantification determined 2 days after last CCl4 injection) | HSC inhibition does not affect proliferation in the tumor compartment | 3.024 | 1.602 | 0.4443 |
| | YAP Δ HSC | | | 3.266 | 1.367 | 0.3652 |
| Ext.Fig. 3n | DTRneg | DEN+14xCCl4 (DT: late depletion) (quantification determined 3 days after last CCl4 injection) | HSC depletion does not affect proliferation in tumor compartment | 0.6126 | 0.3714 | 0.1661 |
| | DTRpos | | | 0.7705 | 0.4297 | 0.1432 |



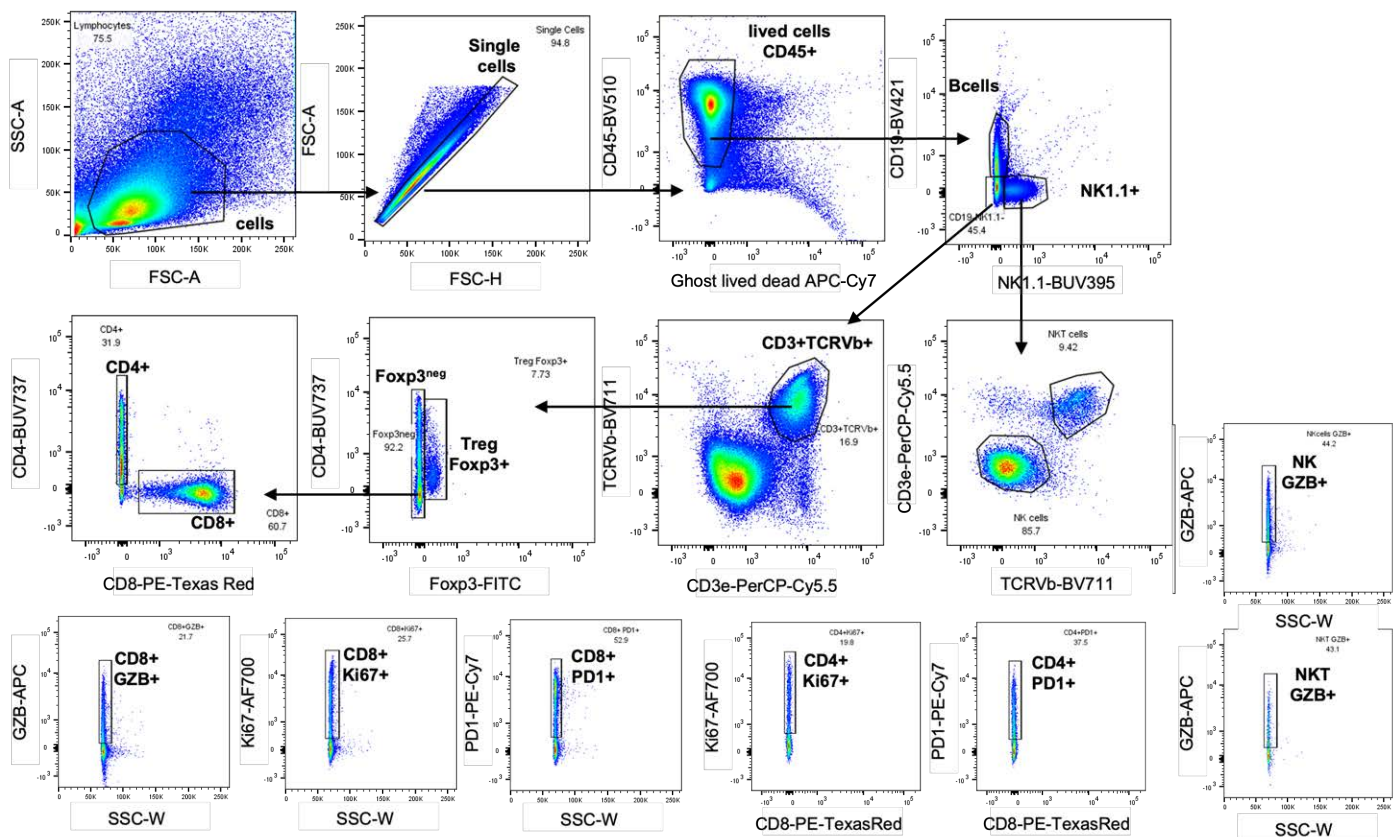
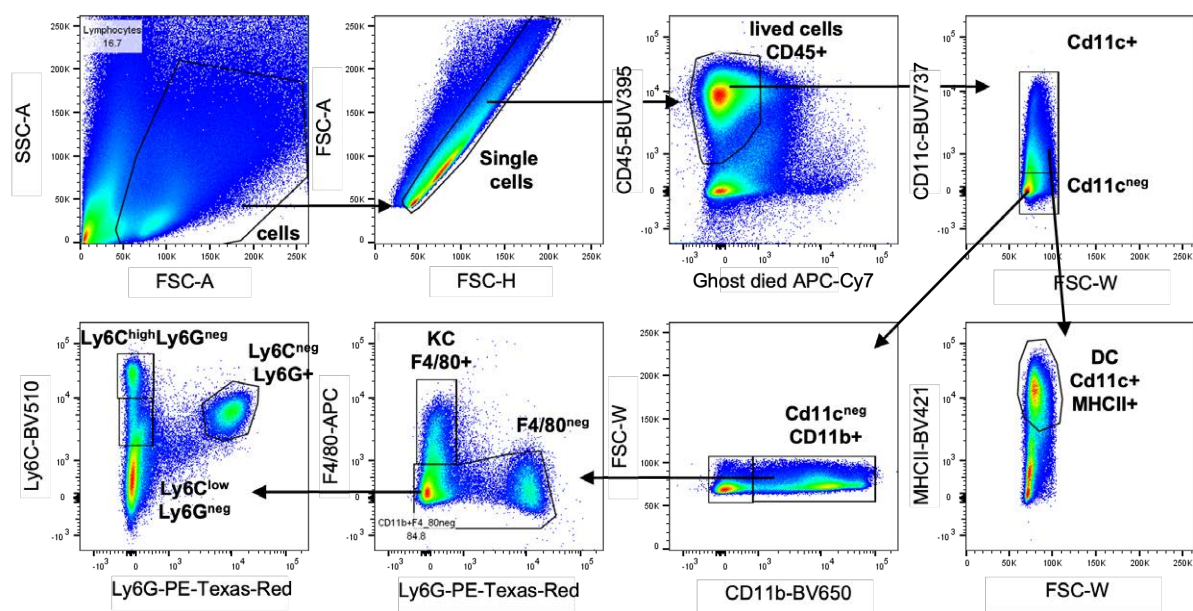
Supplementary Information 1| Single nucleus RNA-sequencing analysis of human normal, fibrotic and HCC liver tissues. **a**, UMAP visualization of sn-RNAseq of human livers shows cell repartition of normal (n=4), cirrhotic (n=4) NASH patients, among those n=2 from NASH-HCC non-tumor tissue) and HCC (n=2 NASH-HCC) cases. **b**, Clusters (upper left panel) were analyzed to determine cell populations (lower left panel) using specific markers for each cell types (dot plot, upper right panel); the square insert shows the fibroblast population. **c**, UMAP visualization of the different fibroblast populations (left panel) and only the HSC cluster with the repartition of patients (middle panel) and normal (n=4) or cirrhotic (n=4) cases (right panel). Myelo: myeloid cells, Endo: Endothelial cells, Prolif: proliferative, Cholangio: cholangiocytes.

a**b**

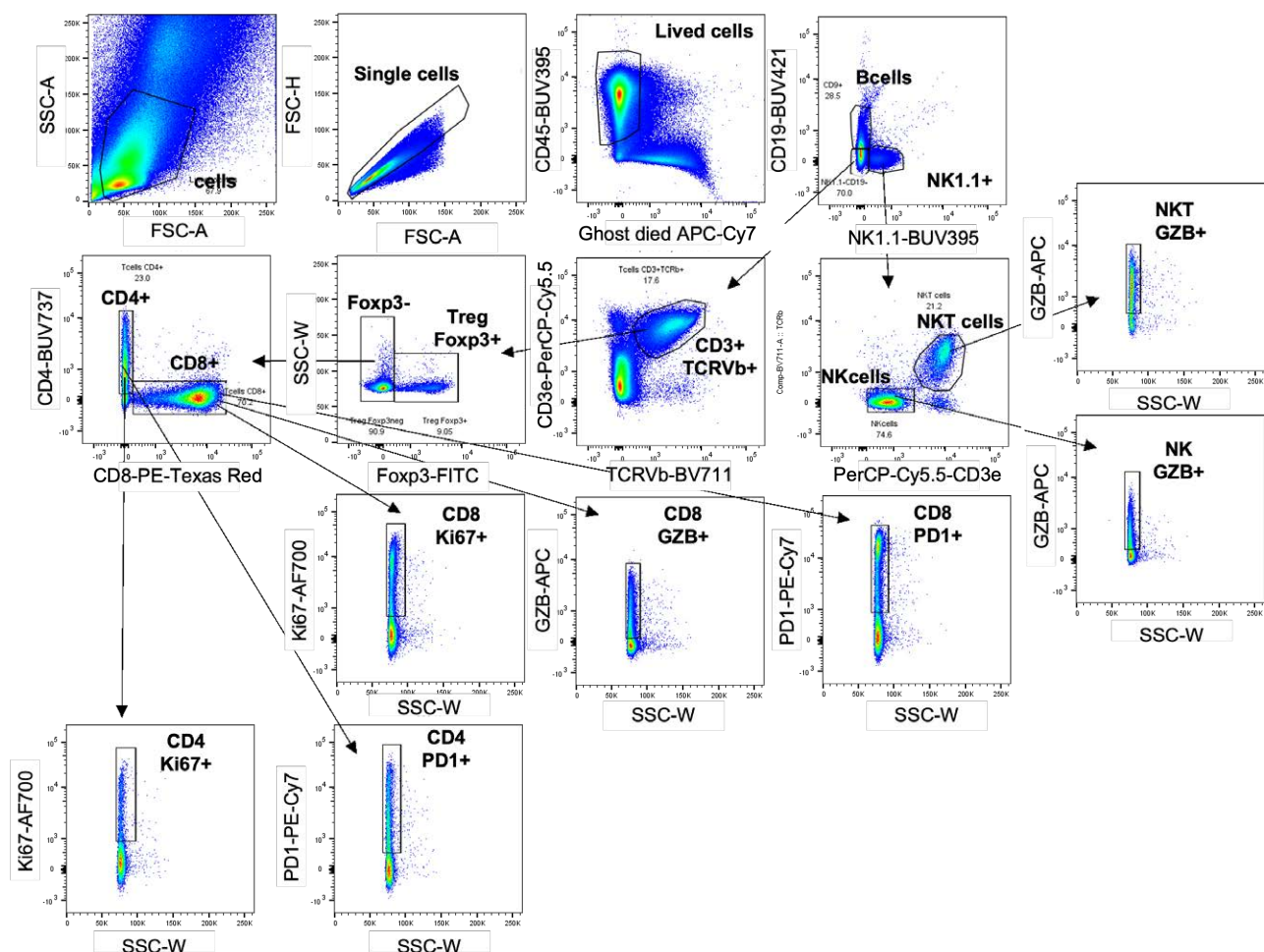
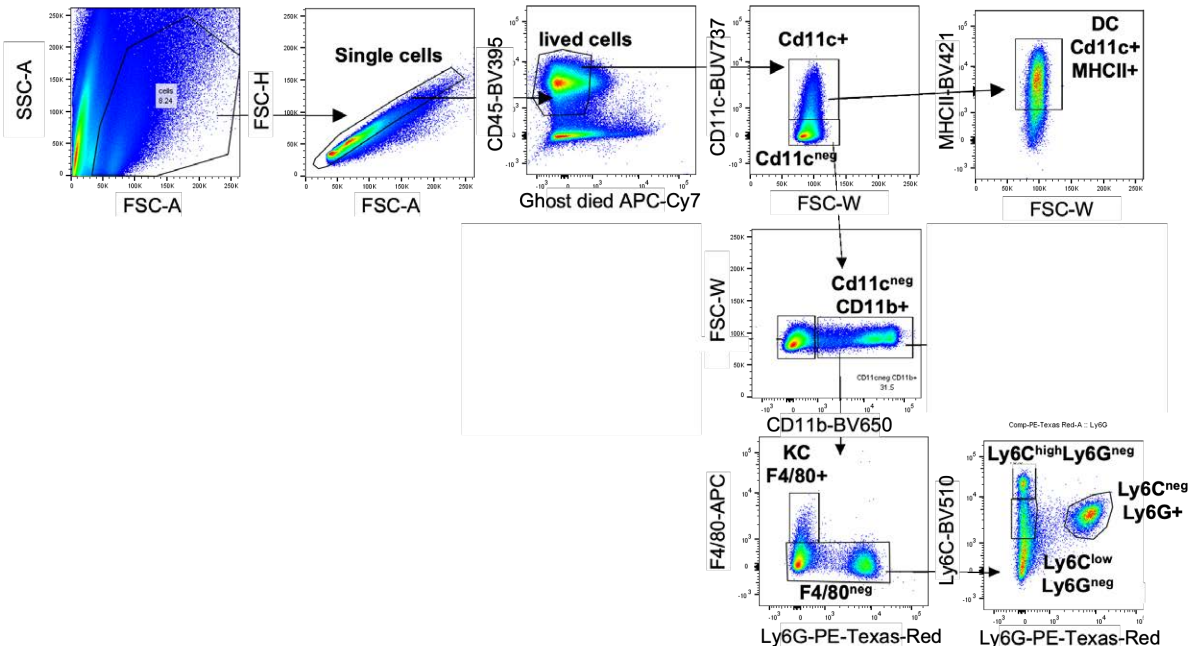
Supplementary Information 2 | Immune cell analysis by flow cytometry in the fibrotic liver or HCC from mice with genetic HSC depletion or inhibition. a-b Gating strategy used to analyse lymphocyte (a) and myeloid (b) cells population in the non-tumour and HCC tissues from α SMA-Tk^{neg} and α SMA-Tk^{pos} mice treated with DEN+CCl₄ (analysis related to Extended Data Figure 4h). NK: Natural Killer, NKT: NK T cells, KC: Kupffer Cell and DC: Dendritic cell



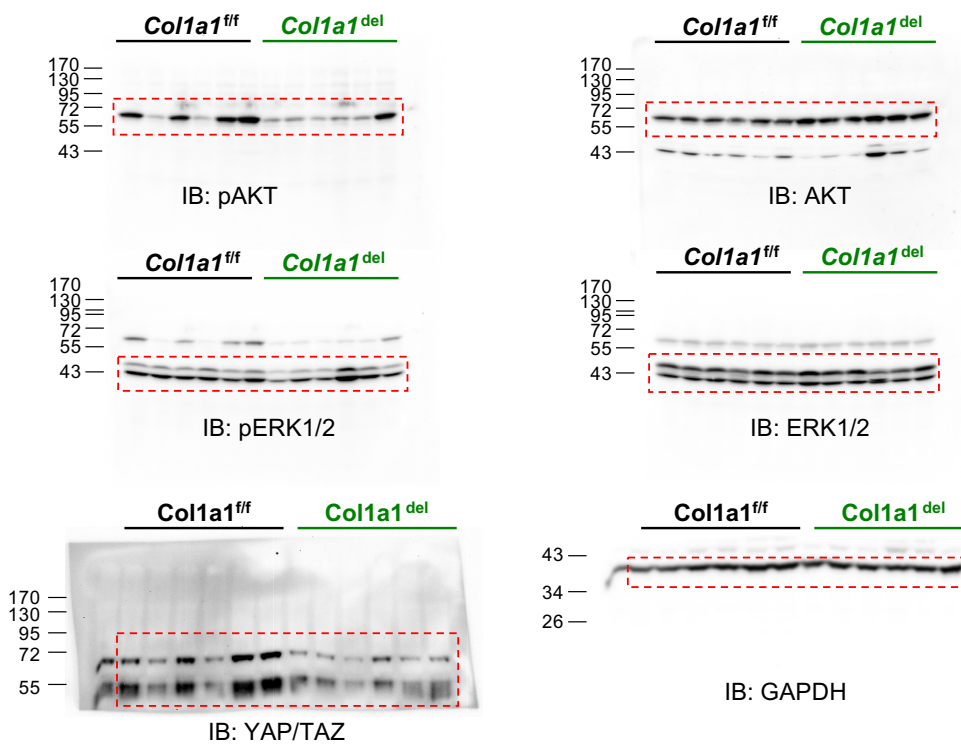
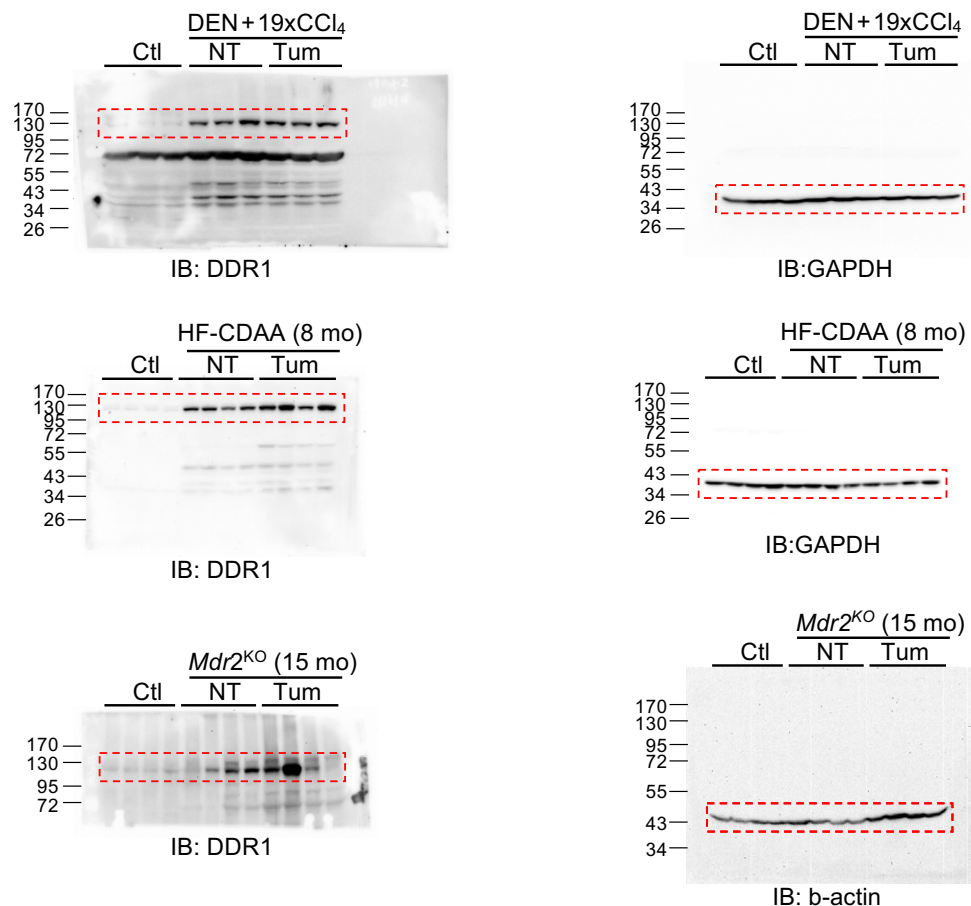
Supplementary Information 3 | Strategy to generate a single cell RNA-sequencing signature for weakly and strongly activated HSC subpopulations. HSC from LratCre+ TdTomato^{homo} mice (a) treated with 19 injections CCl₄ (n=1), (b) TAZ+FPC-diet (n=1) or (c) fed with CDAA-diet for 3 months (n=1) were FACS-sorted based on TdTomato fluorescence and d, Col1a1 expressing cells from 3 month old Mdr2^{KO} Col1a1-GFP+ mice (n=1) were FACS-sorted based on Col1a1-GFP fluorescence. All samples were analyzed by scRNA-sequencing. The HSC population was selected and reclustered based on known HSC markers (*Pdgfra*, *Pdgfrb*, *Dcn*, *Des*, *Colec11* and *Lrat*) and other clusters containing cells expressing proliferative (Prolif), hepatocytes (Hepato), cholangiocytes (Cholangio), Immune, endothelial (Endo), mesothelial (Meso), portal fibroblasts (PF) and vascular smooth muscle cells (VSMC) markers were excluded, as displayed in the dotplots. Next, the HSC cluster with the highest level activation (in purple) or the least activated HSC (in red) were identified using an activation score comprised of activation marker genes *Acta2*, *Lox*, *Col1a1* and *Timp1* using 'AddModuleScore' function and averaging across the cells in the cluster (average score for the clusters with highest and lowest scores are indicated). Highest and least activated clusters were then used to generate common scRNA-signatures to identify highly and less activated HSC (related to Main Fig.3).

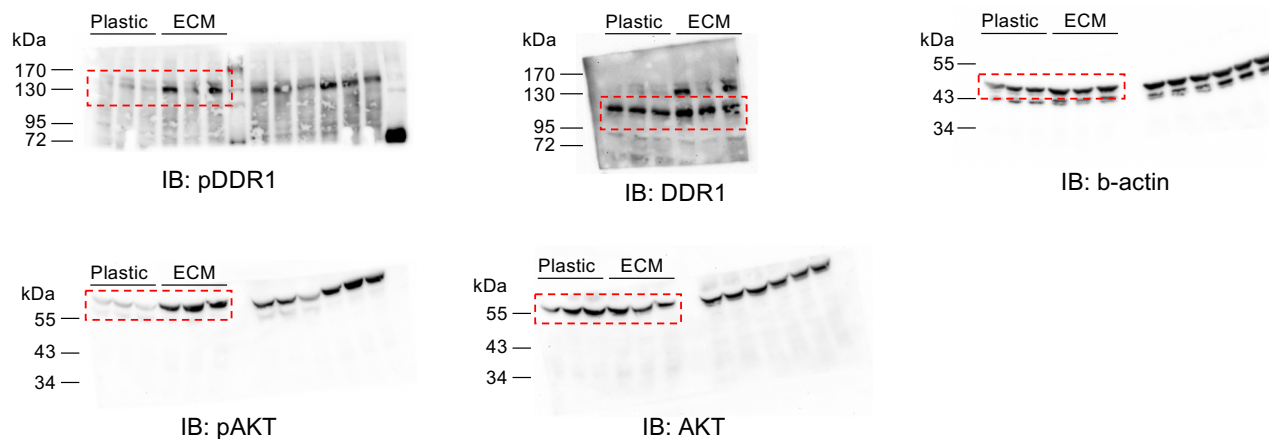
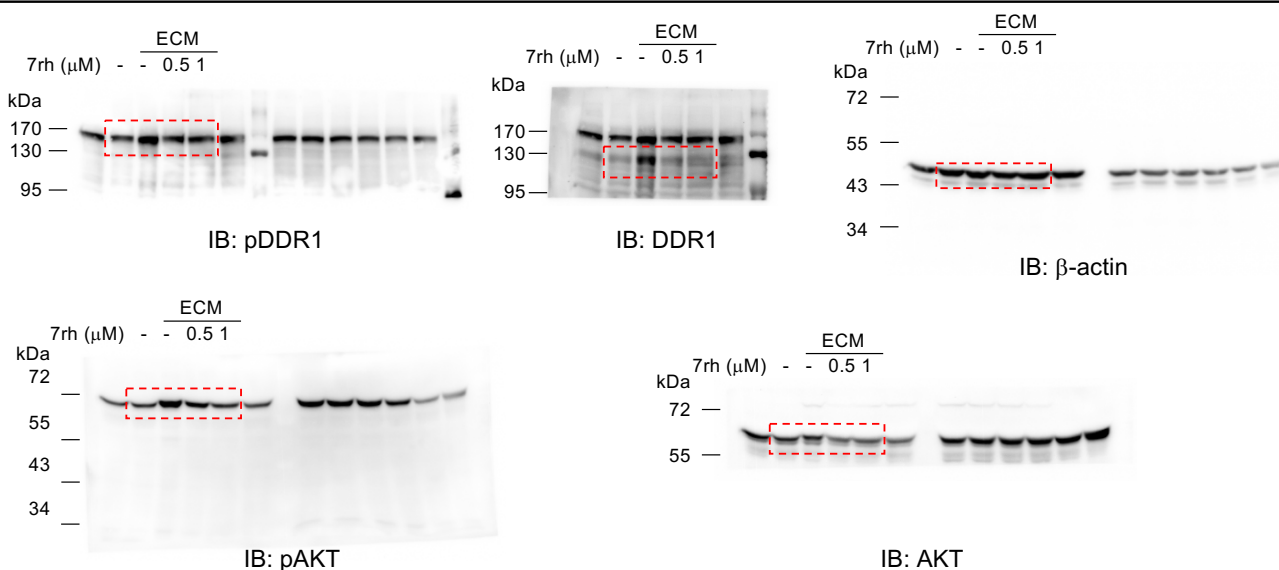
a**b**

Supplementary Information 4| Immune cell analysis by flow cytometry in the fibrotic liver or HCC from mice with genetic deletion of *Co1a1* in HSC. a-b Gating strategy used to analyse lymphocyte (a) and myeloid (b) cells population in the non-tumour and HCC tissues from *Co1a1*^{fl/fl} and *Co1a1*^{ΔHSC} mice treated with DEN+CCl₄ (analysis related to Extended Data Figure 9e-g). NK: Natural Killer, NKT: NK T cells, KC: Kupffer Cell and DC: Dendritic cell

a**b**

Supplementary Information 5| Immune cell analysis by flow cytometry in CCl₄-induced liver injury in the fibrotic liver from mice with deletion of *Hgf* in HSC. **a-b** Gating strategy used to analyse lymphocyte (**a**) and myeloid (**b**) cell population in the fibrotic liver from *Hgf*^{f/f} and *Hgf*^{ΔHSC} mice treated with 6xCCl₄ (analysis related to Extended Data Figure 12g). NK: Natural Killer, NKT: NK T cells, GZB: granzyme B, KC: Kupffer Cell and DC: Dendritic cell

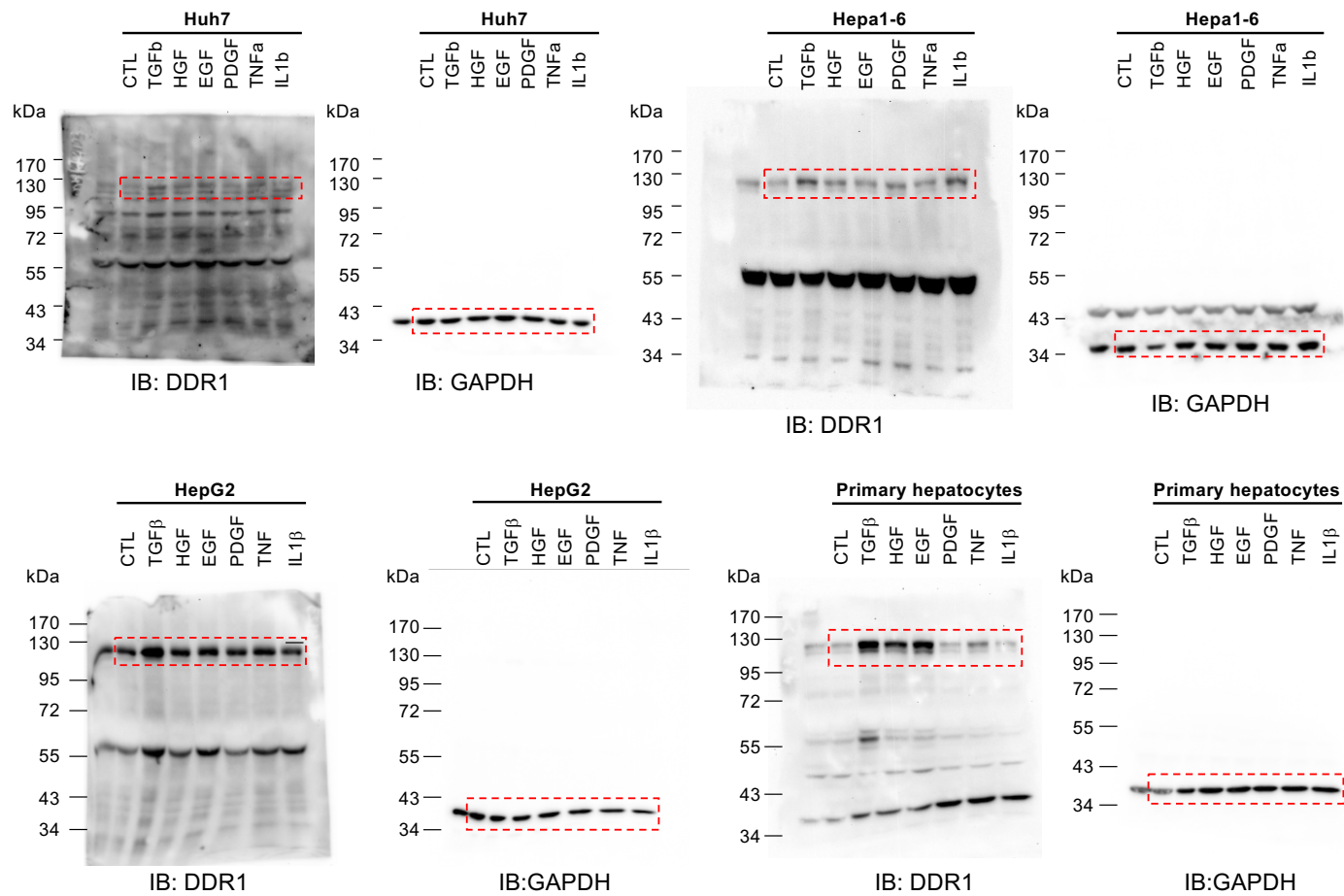
a*Full size immunoblots Figure 4f***b***Full size immunoblots Figure 5a***Supplementary Information 6|** Uncropped immunoblots from Main Figures 4f (a) and Mine Figure 5a (b).

a*Full size immunoblots Figure 5e***b***Full size immunoblots Figure 5f***c***Full size immunoblots Extended Data Figure 2g*

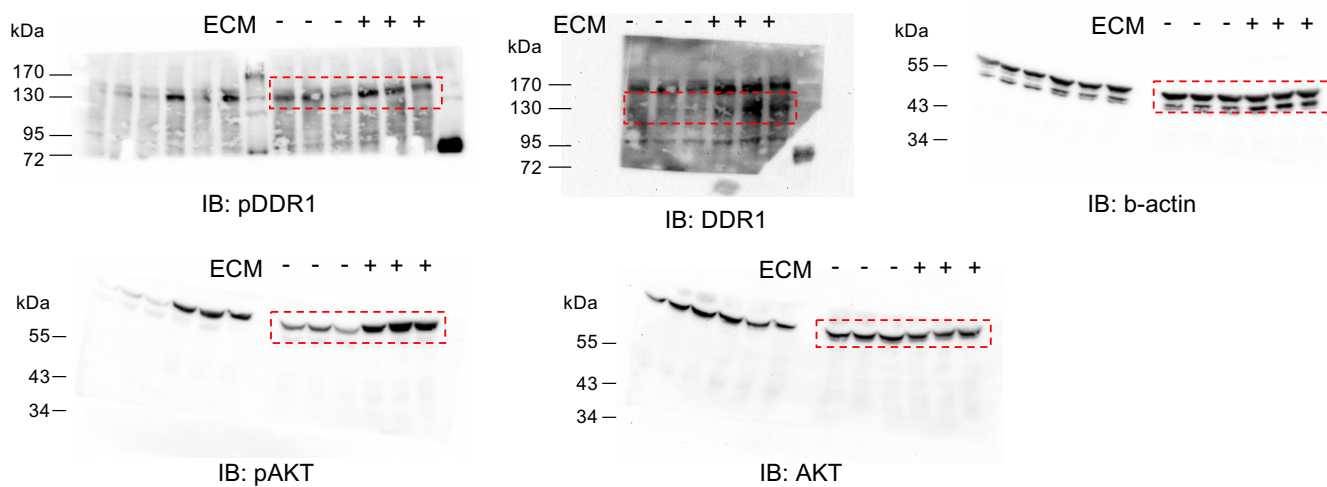
Supplementary Information 7| Uncropped immunoblots from Main Figure 5e (a), Main Figure 5f (b) and Extended Data Figure 2g (c).

a

Full size immunoblots Extended Data Figure 10b

**b**

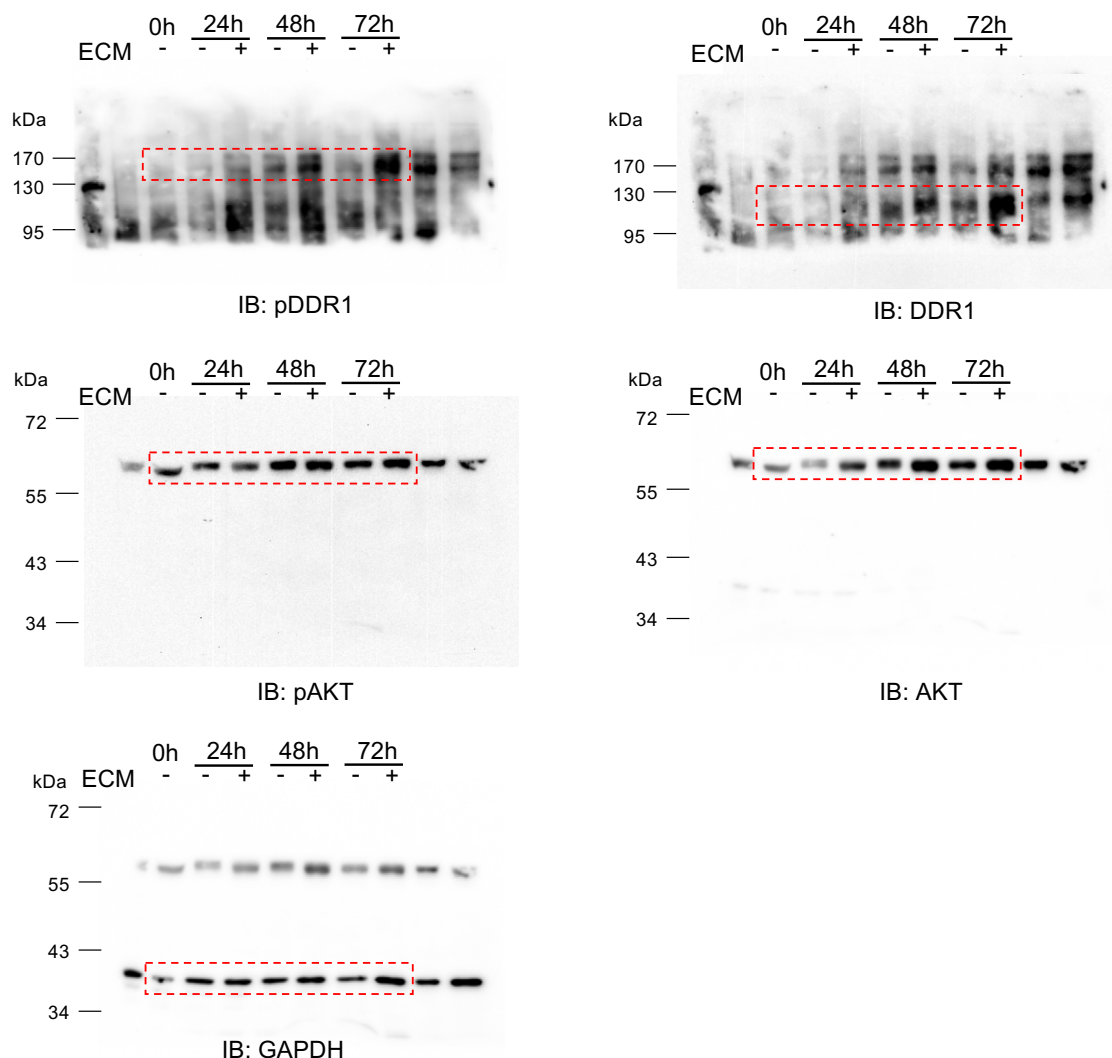
Full size immunoblots Extended Data Figure 10b



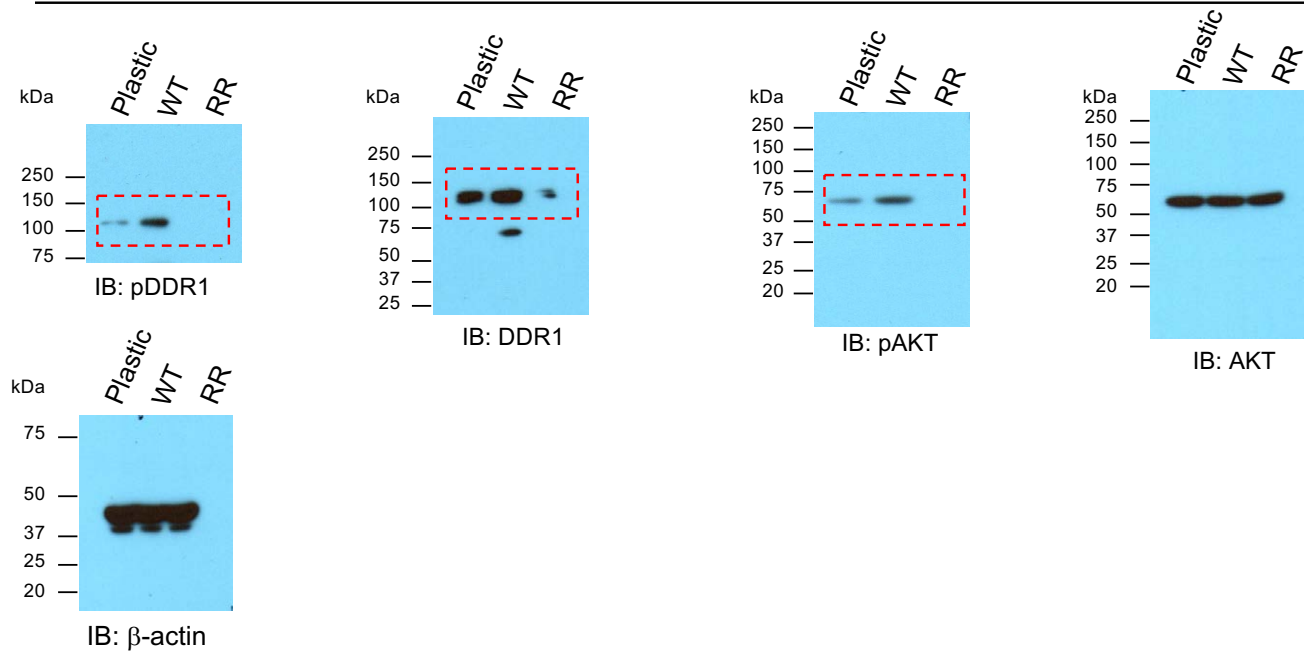
Supplementary Information 8| Uncropped immunoblots from Extended Data Figure 10b (a) and Extended Data Figure 10e (b).

a

Full size immunoblots Extended Data Figure 10f

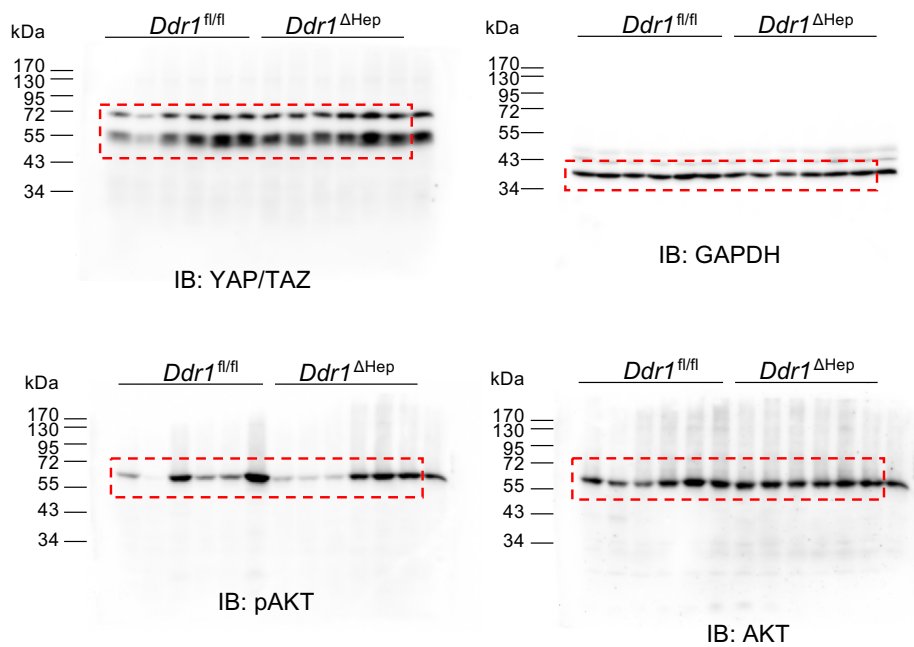
**b**

Full size immunoblots Extended Data Figure 10g



Supplementary Information 9| Uncropped immunoblots from Extended Data Figure 10f (a) and Extended Data Figure 10g (b).

Full size immunoblots Extended Data Figure 10j



Supplementary Information 10| Uncropped immunoblots from Extended Data Figure 10j.